AD_____

CONTRACT NO: DAMD17-89-C-9032

TITLE: MODULATION OF IONIC CHANNEL FUNCTION BY PROTEIN PHOSPHORYLATION

PRINCIPAL INVESTIGATOR: Mauricio Montal

CONTRACTING ORGANIZATION: University of California, San Diego
Department of Biology
9500 Gilman Drive
La Jolla, CA 92093-0319

REPORT DATE: November 12, 1992

TYPE OF REPORT: Final Report

PREPARED FOR: U.S. Army Medical Research and Development Command, Fort Detrick
Frederick, Maryland 21702-5012

DISTRIBUTION STATEMENT: Approved for public release; distribution unlimited

The findings in this report are not to be construed as an official Department of the Army position unless so designated by other authorized documents.

SECURITY CLASSIFICATION OF THIS PAGE

REPORT DOCUMENTATION PAGE

Form Approved OMB No. 0704-0188

1a. REPORT SECURITY CLASSIFICATION: Unclassified	1b RESTRICTIVE MARKINGS
2a. SECURITY CLASSIFICATION AUTHORITY	3 DISTRIBUTION/AVAILABILITY OF REPORT: Approved for public release; distribution unlimited
2b. DECLASSIFICATION/DOWNGRADING SCHEDULE	
4. PERFORMING ORGANIZATION REPORT NUMBER(S)	5. MONITORING ORGANIZATION REPORT NUMBER(S)
6a. NAME OF PERFORMING ORGANIZATION: Regents of the University of California; 6b. OFFICE SYMBOL (If applicable)	7a. NAME OF MONITORING ORGANIZATION
6c. ADDRESS (City, State, and ZIP Code): University of California San Diego, 9500 Gilman Drive, La Jolla, CA 92093-0319	7b. ADDRESS (City, State, and ZIP Code)
8a. NAME OF FUNDING/SPONSORING ORGANIZATION: U.S. Army Medical Research & Development Command; 8b. OFFICE SYMBOL (If applicable)	9. PROCUREMENT INSTRUMENT IDENTIFICATION NUMBER: DAMD17-89-C-9032
8c. ADDRESS (City, State, and ZIP Code): Fort Detrick, Frederick, MD 21702-5012	10 SOURCE OF FUNDING NUMBERS

PROGRAM ELEMENT NO.	PROJECT NO.	TASK NO.	WORK UNIT ACCESSION NO
61102A	3M1-61102BS12	AA	WUDA318142

11. TITLE (Include Security Classification): Modulation of Ionic Channel Function by Protein Phosphorylation

12. PERSONAL AUTHOR(S): Mauricio Montal

13a. TYPE OF REPORT	13b. TIME COVERED	14. DATE OF REPORT (Year, Month, Day)	15. PAGE COUNT
Final	FROM 3/15/89 TO 10/14/92	1992 November 12	52

16. SUPPLEMENTARY NOTATION

17. COSATI CODES		
FIELD	GROUP	SUB-GROUP
06	02	
06	01	

18. SUBJECT TERMS (Continue on reverse if necessary and identify by block number): Protein phosphorylation/ion channels; RA1

19. ABSTRACT (Continue on reverse if necessary and identify by block number)

Protein phosphorylation is considered a key event in synaptic physiology. The acetylcholine receptor (AChR), a prototype of ligand-gated ion channels, plays a central role in postsynaptic signal transduction. To examine the functional consequences of AChR phosphorylation, single-channel properties of purified *Torpedo californica* AChR reconstituted in planar lipid bilayers, were evaluated before and after phosphorylation by purified protein-serine and -tyrosine kinases, or dephosphorylation by recombinant protein tyrosine phosphatase. Single-channel conductance was not altered by changing the AChR serine or tyrosine phosphorylation state. In contrast, the AChR open-channel probability was markedly affected both by the extent of receptor phosphorylation in different subunits and by agonist concentration. Notably, the spontaneous open-channel probability of serine-phosphorylated AChRs is significantly higher than that of AChRs phosphorylated on tyrosine residues or of unphosphorylated AChRs. Channel activation by protein kinase A and protein kinase C is correlated with AChR phosphorylation and is abolished by α-bungarotoxin. Thus, phosphorylation on
(cont. on reverse)

20. DISTRIBUTION/AVAILABILITY OF ABSTRACT	21. ABSTRACT SECURITY CLASSIFICATION
☐ UNCLASSIFIED/UNLIMITED ☒ SAME AS RPT. ☐ DTIC USERS	

22a. NAME OF RESPONSIBLE INDIVIDUAL	22b. TELEPHONE (Include Area Code)	22c. OFFICE SYMBOL
Mary Frances Bostian	301-619-7321	SGRD-RMI-S

DD Form 1473, JUN 86 — Previous editions are obsolete. — SECURITY CLASSIFICATION OF THIS PAGE

19. ABSTRACT (continued)

serine residues of γ and δ subunits activates AChR channel opening in absence of ligand binding. In presence of acetylcholine (ACh), open-channel probability is augmented displaying the most significant effect at lower ACh concentrations. The increment of open-channel probability for ACh-activated channels arises from an increase in the opening frequency and a shortening of the characteristic long quiescent periods that separate the bursts of channel openings. In contrast, AChRs phosphorylated on tyrosine residues were not activated in absence of ACh and open-channel probability was differentially modulated both by the extent of receptor phosphorylation and by agonist concentration. At ≤ 1μM ACh, AChR phosphorylation increased the open probability arising from an increment in the frequency of events and a concomitant prolongation of channel open lifetime. At > 1 μM ACh, however, a remarkable decrease of channel activity was measured after phosphorylation. Thus, tyrosine phosphorylated AChRs feature a higher sensitivity to ACh and activate and desensitize at lower concentrations than those required by unmodified or dephosphorylated receptors. It is plausible, therefore, that the functional response of the receptor *in vivo* depends on the specific phosphorylation site that is covalently modified. A complementary strategy involved the use of recombinant DNA technology to delete and mutate serine and threonine residues in the*Torpedo californica* AChR β, γ and δ subunits.known to be modified by the activity of protein kinases in the The gene products of the wild-type and mutant cDNAs were expressed in *Xenopus laevis* oocytes and their activity characterized electrophysiologically. No consistent pattern of modifications emerged from the analysis. Therefore, a structurally simpler neuronal AChR α7 was pursued. AChR α7 is a homomeric receptor channel that, in contrast to the neuromuscular AChR which is composed of four different subunits with nine distinct potential phosphorylation sites, contains a single consensus phosphorylation site for protein kinase A. Point mutations of this site, serine 344, were engineered in which serine was replaced by alanine, threonine, aspartic acid, asparagine, glutamic acid or glutamine. Wild-type and mutant gene products were expressed in oocytes. The serine to glutamic acid mutants displayed the most striking effect: activation by ACh at higher agonist concentration and a slower rate of desensitization. Significantly, the serine to glutamine mutation reversed these effects, whereas the serine to alanine mutant was indistinguishable from the wild-type. Chimeric constructs consistent of the AChR α7 with an insertion of the cytoplasmic 22-residue domain containing the putative phosphorylation site of the neuromuscular-type AChR subunits were generated, and the electrophysiological activity of the gene products analyzed after expression in oocytes. The chimeric constructs implanted with the phosphorylation motif of the β and δ subunits displayed significantly lower current response amplitudes at all ACh concentrations tested. The role of protein phosphorylation was evaluated on the human cerebellar medulloblastoma cell line TE671. Patch clamp recordings, obtained in the cell attached and whole cell configurations, showed no significant effects under conditions inferred to result in AChR phosphorylation. Taken together, our results show that ligand binding and protein phosphorylation concertedly regulate the conformational transitions of the AChR that lead to the channel open and desensitized states. AChR phosphorylation provides, therefore, a mechanism to optimize both response activation and termination, and may have functional significance for the plasticity of cell-cell communication in the nervous system. Parallel studies on voltage-gated sodium channels led to the isolation of the first cDNA clone for a human brain voltage-gated sodium channel, denoted as HBA. The gene product was expressed by transfection in mammalian cells. Expressed HBA currents were voltage-dependent, sodium-selective and tetrodotoxin-sensitive and, thus, exhibit the biophysical and pharmacological characteristics of sodium channels.

FOREWORD

Opinions, interpretations, conclusions and recommendations are those of the author and are not necessarily endorsed by the U.S. Army.

___X___ Where copyrighted material is quoted, permission has been obtained to use such material.

___X___ Where material from documents designated for limited distribution is quoted, permission has been obtained to use the material.

___X___ Citations of commerical organizations and trade names in this report do not constitute an official Department of Army endorsement or approval of the products or services of these organizations.

___X___ In conducting research using animals, the investigator(s) adhered to the "Guide for the Care and Use of Laboratory Animals," prepared by the committee on Care and Use of Laboratory Animals of the Institute of Laboratory Resources, National Research Council (NIH Publication No. 86-23, Revised 1985).

___X___ For the protection of human subjects, the investigator(s) adhered to policies of applicable Federal Law 45 CFR 46.

___X___ In conducting research utilizing recombinant DNA technology, the investigator(s) adhered to current guidelines promulgated by the National Institutes of Health.

Accesion For	
NTIS CRA&I	☒
DTIC TAB	☐
Unannounced	☐
Justification	
By	
Distribution /	
Availability Codes	
Dist:	Avail and / or Special
A-1	

N. Mootre 11/12/92
PI - Signature DATE

Table of Contents

5. Appendices

1. Introduction

A fundamental event in signal transduction is receptor phosphorylation (1). Protein phosphorylation has been correlated with modulation of receptor activity by either enhancing or terminating the action of the ligand (1,2,3). However, is there a functional modification of membrane receptors in absence of the natural occurring ligand? In this program we have addressed this question by measuring receptor activation directly at the level of single channel currents from purified AChRs reconstituted in planar lipid bilayers. Having characterized in detail the channel properties of the purified AChR, both in terms of ion conduction (4) and of gating kinetics (5-7), we are in a position to identify changes that may arise as a consequence of receptor phosphorylation. The nicotinic cholinergic receptor, especially that purified from *Torpedo* electric organ, is the best characterized neurotransmitter receptor (for reviews see 8-10). The AChR is an integral membrane protein (M_r 250 kDa) composed of four homologous glycoproteins subunits α (40 kDa), β (50 kDa), γ (60 kDa) and δ (65 kDa) with a stoichiometry $\alpha 2\beta\gamma\delta$ (8-10). This membrane receptor is phosphorylated by at least four different protein kinases: i) a cyclic AMP-dependent protein kinase that phosphorylates mainly γ and δ subunits (11-13); ii) a lipid-dependent protein kinase C that covalently modifies δ subunits (14); iii) a Ca^{2+}/calmodulin protein kinase II that incorporates phosphate in β and δ subunits (15), and iv) a tyrosine-specific protein kinase which phosphorylates β, γ and δ subunits (16,17). The physiological role of AChR phosphorylation remains unclear.

Single-channel recordings, under non-steady state conditions, from purified AChR reconstituted in liposomes suggested a role for tyrosine phosphorylation in regulating a fast component of receptor desensitization (17). Similar conclusions were inferred from fast-flux measurements after AChR phosphorylation on serine residues (12). Conversely, AChR channel activity measured under steady-state conditions demonstrated that protein serine phosphorylation increases both the spontaneous (18) and the ACh-evoked activity of the AChR (19). Together, the results suggest that both AChR activation and desensitization are controlled by phosphorylation/dephosphorylation events. Here, we characterize the modification of AChR channel activity by specific protein tyrosine phosphorylation and dephosphorylation under steady-state conditions. The approach involves the use of purified recombinant protein tyrosine kinases and phosphatases to assess the specificity and reversibility of this covalent modification on purified *Torpedo californica* AChR reconstituted in lipid bilayers, while excluding effects of other cellular modulators. Results show a tight coupling between the extent of AChR tyrosine phosphorylation and the efficacy of ACh to open the receptor channel. This analysis suggests that regulation of AChR channel gating depends on a concerted interplay between two interacting mechanisms, associated with two distant structural domains of the protein, the ACh binding site exposed to the synaptic cleft and the phosphorylation domain limited to the cytosol.

To assess the contribution of a single subunit in the AChR $\alpha 2\beta\gamma\delta$ complex to the phosphorylation effect, the modification provided by protein kinase C, which modifies δ subunits was investigated.

A complementary strategy involved the use of recombinant DNA technology on a structurally simpler AChR than that present in the neuromuscular junction, namely the neuronal $\alpha 7$ gene product (AChR$\alpha 7$) (20,21). Site-directed mutagenesis was performed to exchange the potential phosphorylation site of the AChR$\alpha 7$, serine-344, for alanine, glutamic acid, aspartic acid, threonine, glutamine and asparagine. "Cassette-mutagenesis" was used to create chimeric $\alpha 7$ implanted with the cytoplasmic 22 amino acid segment containing the putative phosphorylation site of the muscle-type AChR subunits. Wild-type, mutants and chimaeras were expressed in *Xenopus laevis* oocytes for functional analysis. Macroscopic ACh-elicited currents properties (activation and desensitization kinetics, agonist dependence, voltage dependence and ionic selectivity) were characterized. A similar program involved studies on voltage-gated sodium channels.

2. Body
2.1 Experimental Methods

AChR purification and reconstitution in lipid vesicles. Receptor from the electric organ of *Torpedo californica* (Pacific Bio-Marine Labs, Inc. Venice, CA) was solubilized, purified and reconstituted in soybean lipid vesicles (32 mg/ml) supplemented with cholesterol (8 mg/ml) and assayed as described (8). Final AChR concentration in the vesicles was 4.0 μM. Binding sites for a-bungarotoxin (BGT) were equally distributed between the interior and exterior of reconstituted vesicles (4,8).

Planar lipid bilayers at the tip of a patch pipet. Lipid vesicles containing AChR (1.5 μl) were diluted in 200 μl of buffered salt medium composed of 0.5 M KCl, 8 mM $CaCl_2$, 15 mM $MgCl_2$, 50 μM 4,4'-diisothiocyanatostilbene-2,2'-disulfonic acid (DIDS), 10 mM Hepes (pH 7.4) and mixed for 20 sec. DIDS is used to block a Cl^- channel that may copurify with AChRs (7). Suspensions were incubated 20 min and transferred to bilayer chambers for electrical recordings. Planar lipid bilayers were formed at the tip of patch pipets by apposition of monolayers derived from AChR vesicles as described (4,7,8,22). This procedure to form bilayers dictates the occurrence of two populations of oriented AChRs with (ACh binding sites facing the interior of the pipet or the external bath solution (8,22). If indicated, the AChR channel was activated by 1μM ACh present inside the pipett which contained the buffered salt medium. In this configuration, the population of AChRs that possess the ACh binding sites exposed to the pipet interior is functionally selected (8,22). All experiments were conducted at 22 ± 2°C.

Data acquisition and analysis. Single-channel recordings and data processing were done as described (4-7) using an Axon TL-1 interface (Axon Instruments, Inc., Burlingame, CA) connected to a 386-based computer. Data were processed using the pClamp 5.5 package (Axon Instruments). Records were filtered at 5 kHz and digitized at 10 kHz. Records in which only one channel was open at any given time were filtered at 1 kHz, or as indicated otherwise, using a gaussian filter and analyzed. Open probability was calculated by integration of conductance histograms (4-7) or from dwell time histograms (23) according to : $P_O = N\,\tau_O/T$, where N is the number of transitions, τ_O is the mean open time, and T is the total recording time. The results are equivalent. Histograms of dwell times in the open state were well fitted by a probability density function of the form $N(t) = A_S\exp(-t/\tau_S)+A_L\exp(-t/\tau_L)$ using a χ^2 minimization algorithm (6,7). Subscripts S and L denote the short and long components of the distribution. Data were filtered at 1 kHz, or as otherwise indicated, and openings shorter than 0.25 ms were ignored (7). In all cases, data are well fitted by a sum of two exponentials adopting a 5% significance level.

***In vitro* phosphorylation of AChR by kinase A.** AChR phosphorylation was conducted *in vitro* in a final volume of 100 μl containing 15 μg of AChR protein in reconstituted vesicles, 10 mM $MgCl_2$, 0.1 mM EGTA, 20 mM Hepes (pH 7.4), 1 μg of recombinant purified protein kinase A from murine heart (24), 9.6 nmol of unlabeled ATP with 0.76 nmol of [γ-^{32}P]ATP. Reactions proceeded at 22°C on a horizontal shaker and were terminated by addition of 150 ml of 0.1 M EDTA, pH 8.0. Suspensions were centrifuged in the airfuge (Beckman Instruments) for 20 min at 30 psi (1 psi = 6.9 kPa). The same procedure was applied for control vesicles, in which either protein kinase A and/or ATP, or both were omitted. Pelleted material was subjected to electrophoresis on SDS/10% polyacrylamide gels (25). Gels were stained with Coomassie blue, destained, dried on Whatman 3 MM filter paper and exposed to Kodak X-Omat AR x-ray film. For quantitation of ^{32}P incorporated, protein bands were cut and assayed in scintillation fluid (Filtron-X, National Diagnostics, Manville, NJ). The stoichiometries reported were calculated on the basis of a 50% orientation of AChRs in the reconstituted vesicles (8), namely, that 50% of the

receptors had the ACh binding sites accessible to the bathing media. Identical protocols were used to prepare samples for electrical recordings but [γ-^{32}P]ATP was omitted. Pellets were resuspended in 230 ml of buffered salt medium composed of 0.5 M KCl, 5 mM $CaCl_2$, 0.5 mM 4,4'-diisothiocyanatostilbene-2,2'-disulfonic acid, 10 mM Hepes (pH 7.4) and transferred to bilayer chambers for electrical recording as described above.

AChR tyrosine phosphorylation and dephosphorylation. AChR phosphorylation by recombinant and purified human protein tyrosine kinase p60$^{c\text{-}src}$, denoted as PTK, (Oncogene, Uniondale, NY) was performed in 210 µl containing 50 µg of AChR protein in lipid vesicles, 500 mM KCl, 5 mM $CaCl_2$, 10 mM $MgCl_2$, 10 mM HEPES pH 7.4, 0.1% β-mercaptoethanol, 250 µM ATP, and 20 U/ml of PTK. AChR dephosphorylation by purified tyrosine phosphatase PTPase 1B, the catalytic segment of protein phosphatase CD45 from human placenta (5 U/ml), denoted as PTP, (26) was conducted under similar conditions, except for the omission of $MgCl_2$ and ATP from the reaction mixture. The stoichiometry of receptor tyrosine phosphorylation was obtained using identical protocols but the reaction mixture was supplemented with 3 µCi of [γ-^{32}P] ATP (Amersham, Arlington Heights, IN). Radioactive samples were processed as described (18). The enzymatic reactions proceeded for 30 min. To terminate the PTK and PTP treatments, 12 mM EGTA/KOH pH 7.4 or 100 mM $(NH_3)_6Mo_7O_{24}$ were used, respectively. When indicated, recombinant catalytic subunit of protein kinase A from murine heart (24) was 0.065 U/ml and purified protein kinase C from rat brain (Calbiochem, San Diego, CA) was 1.5 U/ml. β-mercaptoethanol was omitted from the protein kinase A phosphorylation mixture.

Phosphotyrosine detection by immunoblot analysis. AChR subunits were separated by SDS/PAGE (10%) electrophoresis (25) and transferred to nitrocellulose membranes using a semi-dry blotter (27). Protein tyrosine phosphorylation was detected by immunoblot analysis using monoclonal antibodies against phosphotyrosines (Upstate Biotechnology, Inc., New York, NY). Membranes were incubated with an IgG2bk mouse monoclonal antiphosphotyrosine antibody using non-fat skim milk as blocking solution, and a goat antimouse IgG antibody conjugated to alkaline phosphatase as the secondary antibody.

Mutagenesis of *Torpedo* AChR subunits. The *Bam H1* fragments from the β and δ subunits and the *Cla1-Sal1* fragment from the γ subunit expression vector were subcloned into pBluescript SK(-). Mutagenesis was performed on the pBluescript vector according to Kunkel (28). Mutants were first identified by restriction enzyme analysis. For the β and δ mutants *Sca1* and *Ssp1* were eliminated, respectively, whereas for the γ mutant a size difference of the *Cla1-Sal1* fragment was identified. Dideoxy sequencing (29) was conducted to confirm the correct mutations. Thereafter, the mutated fragments were subcloned from pBluescript back into their expression vector pSP64T.

Site-directed mutagenesis of neuronal AChRα7. A cDNA coding for a neuronal α7 receptor from chicken brain in the construct pCH2934-SP6 (20) was kindly provided by Dr. Ralf Schoepfer.

The serine residue, S344 (Figure 21), presumably phosphorylated by kinase A was mutated to A (AChRα7S->A), D (AChRα7S->D), E (AChRα7S->E), Q (AChRα7S->Q), N (AChRα7S->N) and T (AChRα7S->T). DNA sequencing (29) was carried out to confirm the presence of the designed mutations and the absence of stray mutations.

Chimeric AChRα7. Chimeric AChRα7s containing the phosphorylation sites of the muscle-type AChR subunits were obtained using a "cassette-mutagenesis" approach. First, the nucleotide

sequence (nt 1018-1086) coding for the protein domain that contains the putative phosphorylation site (aa340-362) was deleted by oligonucleotide directed *in vitro* mutagenesis as described. An oligonucleotide (5'-GCCTGTCAACATAAACAGCTGCTGATAATTGGGTTT-3'), encompassing 17 nucleotides (nt 1000-1017) in the 5' upstream region preceding aa340 and 17 nucleotides (nt 1087-1104) in the 3' downstream region after aa362, was synthesized and used as a primer. The protocol determines the generation of a unique *Pvu* II restriction site in the deleted region. This site was used to insert oligonucleotides coding for the equivalent amino acid sequences of the muscle-type AChR (Figure 20). Standard subcloning procedures were utilized. This strategy was used to generate chimeric AChRα7, namely AChRα7γ and AChRα7δ. To ensure the insertion of the targeted amino acid sequence and the absence of stray mutations, chimeric a7 receptors were sequenced using the Sequenase kit, and the insert ion confirmed.

Sequence and restriction analysis. DNA sequencing was determined on both strands by the dideoxy nucleotide chain-termination method (29) using the Sequenase kit (U.S. Biochemical Corp.). Nucleotide sequences were analyzed using the Genetics Computer Group (Madison, WI) sequence analysis programs (30). The cDNA inserts were characterized by conventional restriction endonuclease mapping procedures (31).

mRNA preparation. RNA transcripts were prepared from the cloned cDNAs using the SP6 RNA promoter/polymerase system (32) with capping accomplished by priming with cap analogues (33). DNAs for the different subunits were purified by CsCl gradient centrifugation and linearized with restriction enzymes cutting at the end of the DNA to be transcribed. Linearized DNAs were purified on agarose gels and then incubated with SP6 polymerase in the presence of the ribonucleotides. The transcription reaction was initiated by mixing the reactants in a final volume of 50 µl at room temperature in the following sequence: SP6 transcription buffer; 40 mM tris (pH 7.5); 10 mM NaCl; 10 mM dithiothreitol; 6 mM $MgCl_2$; 4 mM spermidine; RNasin at 1000 units/ml; 0.5 mM each of adenosine triphosphate (ATP), cytidine triphosphate (CTP) and uridine triphosphate (UTP) [α-^{32}P]UTP at 80 Ci/mmol; 0.1 mM GTP; 0.5 mM diguanosinetriphosphate; 200 µg/ml linearized DNA template; SP6 polymerase at 150 units/ml. The reaction mixture was incubated at 37°C for 70 min. Template DNA was then removed by incubation with RNAse-free DNAse (1µg) for another 15 min. mRNA was quantitated by determining the radioactivity bound to DE81 filter papers after repeated sequential washes in sodium phosphate buffer, water, and ethanol. The rest of the sample was then extracted once with phenol/$CHCl_3$ and twice with $CHCl_3$. RNA was precipitated with ethanol, resuspended in diethylpyrocarbonate- (DEPC) treated water diluted with 2.5 volume of ethanol and stored at -50°C. An aliquot (1µl) was withdrawn before dilution with ethanol and was subjected to electrophoresis on a formamide acrylamide gel. Gels were exposed to x-ray film.

Expression in *Xenopus* oocytes α-BTX binding and channel current recordings (34-37). Adult female *Xenopus laevis* frogs were anesthetized by immersion in 0.1% ethyl 3-aminobenzoate methasulphonate (tricaine, Sigma) for 30 min. A small incision on either side of the abdomen was used to remove two or three ovarian lobes. Lobes were incubated in normal Barth's solution (mM: NaCl 88, KCl 1, $CaCl_2$ 0.4, $Ca(NO_3)_2$ 0.33, $NaHCO_3$ 2.4, $MgSO_4$ 0.82, HEPES 5, pH 7.4). Oocytes were then defolliculated by incubation in calcium-free Barth's solution containing 1 mg/ml collagenase (Sigma type IV) for 2 hours at room temperature. Thereafter, oocytes were washed twice in normal Barth's solution and kept in 35 mm culture dishes in groups of 20-30 oocytes. For injection, mRNA specific for each one of the four specific AChR subunits in ethanol were combined in a molar ratio of 1:1:1:1. The mixture was centrifuged for 15 min and washed with 70% ethanol. The pellet was resuspended in water at a

final RNA concentration of 0.125 μg/ml. The average volume of mRNA injected was 50 nl per oocyte using the Drummond microinjector (#3-00-510, Drummond Scientific, Broomall, PA.) The injected oocytes were incubated at 22°C for 2-3 days in modified Barth's medium. Injected oocytes are assayed for ACh-evoked current by two-microelectrode voltage clamps (37,38). Briefly, oocytes are transferred to a recording chamber (Volume=0.2 ml) and are continuously perfused (2-4 ml/min) with frog Ringer solution (115 mM NaCl, 2.5 mM KCl, 2 mM $CaCl_2$, 10 mM N-tris[hydroymethyl]-2-aminoethanesulfonic acid, pH 7.4) supplemented with 100 μM niflumic acid and 100 μM flufenamic acid, to block the endogenous Ca^{2+}-activated chloride channel (39), in the presence or absence of the tested agonist or antagonist (38).

Whole-cell currents are recorded under voltage clamp (Turbo TEC 01C, NPI Electronics, Tamm, F.R.G.) with two conventional microelectrodes (0.3-0.8 MΩ in 3 M KCl). Oocytes with large ACh-elicited currents (>0.5 μA at -30 mV) were used to acquire single-channel recordings in a patch clamp using the cell-attached, inside-out, and outside-out configurations (37,40). The vitelline envelope was carefully removed by immersing the oocytes for 10-20 min in a hypertonic solution (mM: Kaspartate 200, KCl 20, $MgCl_2$ 1, EGTA 10, HEPES 10, pH 7.4, osmolarity 475 mosm). Glass pipets (Corning glass 7052) were fabricated with a programmable puller (Model P-87, Sutter Instruments, Novato, CA.) to obtain tip resistances of 3-5 Mohm in 150 mM NaCl. Single-channel recordings were acquired and analyzed, as described before, for the lipid bilayers. Recording solutions for both the bath and the pipet were as follows, unless otherwise indicated (in mM: NaCl 140, KCl 3, $CaCl_2$ 2, HEPES 10, 10 glucose, pH 7.3, 300 mosm). For the assay of the toxin binding activity, intact oocytes were incubated at room temperature for 75 min with 8nM ^{125}I- α- BTX (118 cpm/fmol). Oocytes were then washed four times with Barth's solution and radioactivity was counted in a gamma counter. For Control 1, oocytes were incubated for 30 min in the presence of cold toxin (1.2 μM) prior to the addition of labeled toxin. For Control 2, mRNAs were omitted from the injection solution.

Electrical recordings from TE671 human cerebellar medulloblastoma cells. Cells were grown and studied as described in detail previously (41,42). Cells were suitable for experiments between 4 hours and 3 days after harvesting. Records were obtained by the patch clamp technique using the whole-cell and cell-attached configurations. Capacitance transient neutralization and series resistance compensation were carefully optimized using the internal circuitry of the List EPC-7 amplifier. The composition of the bath solution was (in mM): 145 NaCl, 2 $MgCl_2$, 2 $CaCL_2$, 5 KCl, 10 HEPES, 10 glucose, pH was adjusted to 7.3 with NaOH, and mannitol was added to adjust osmolarity to 330 mOsm/l. The pipet filling solution contained (in mM): 140 KCl, 5 EGTA, 2 $MgCl_2$, 10 HEPES, 10 glucose, pH 7.3 adjusted with KOH. ACh and other reagents were applied using a multibarreled perfusion system (43). All experiments were performed at room temperature (22-24°C).

2.2 Results

Spontaneous AChR channel activity is modulated by protein kinase A. Single-channel currents recorded from lipid bilayers containing purified receptor are shown in Fig. 1. A segment of a continuous record obtained in the absence of ACh before and after addition of kinase A and ATP to the bath solution is displayed in Fig. 1A (Upper). Presumably, only those AChRs with their cytoplasmic domain accessible to the kinase and ATP are modifiable. Initially, the record is characterized by the sporadic occurrence of events with very brief duration, barely discerned at this resolution. After addition of kinase A and ATP, a drastic increment in the number of openings and of their lifetime is evident. This is clearly recognized in the lower traces, which display at higher resolution the sections of the records indicated by the arrows. To quantitate this effect, the frequency of openings was determined and, as illustrated in Fig. 1B, it increased 50-fold after kinase A addition. The increased open probability appears to arise from an increment in

the number of openings and from a prolongation of channel open time. The single-channel conductance (γ) is not altered, as indicated in the high resolution records displayed in Fig. 1C and D: γ is 44 pS before and after protein kinase A addition. Channel activation required the simultaneous presence of kinase, ATP and Mg^{2+}; omission of any of these three reactants prevented channel activation.

Modifications of AChR channel activity correlate with the extent of protein serine phosphorylation. To correlate the extent of channel activation produced by protein kinase A with that of AChR phosphorylation, AChRs were first phosphorylated *in vitro* by protein kinase A to specific stoichiometries, then reconstituted in planar bilayers for single-channel characterization, and prepared for autoradiographic staining; this is shown in Figs. 2 and 3. Incubation of purified AChRs reconstituted in phospholipid vesicles with protein kinase A, ATP and $MgCl_2$ results in preferential phosphorylation of the AChR γ and δ subunits (Fig. 2; Right; Fig. 3). In addition, a faint broad band of apparent M_r 45,000, corresponding to proteolytic products of the γ subunit were labeled (11). Western blot analysis of equivalent gels probed with antisera raised against individual subunits of *Torpedo* AChR confirmed that the assigned AChR subunits were phosphorylated by protein kinase A. Figure 3 illustrates the resulting pattern at different stoichiometries of phosphorylation from 0.1 to 1.0 mol phosphate/mol AChR, underscoring the progressive labeling of γ and δ subunits. No phosphoproteins were detected in the control reconstituted AChR vesicles, which were prepared under identical conditions to the phosphorylated vesicles but in the absence of kinase.

Protein-serine phosphorylation of AChR modulates the probability of channel opening. Figure 4 displays corresponding single-channel current recordings. In absence of agonist (Fig. 4A), the spontaneous activity is characterized by the infrequent occurrence of very brief openings. The probability of channel opening, P_o, is 0.08% (Fig. 5A, Table 1). This value is in quantitative agreement with measurements on unmodified AChRs in cultured embryonic mouse skeletal muscle (44,45). The spontaneous activity of AChRs phosphorylated by kinase A to a stoichiometry of 0.3 mol of phosphate per mol of AChR is shown in Figs. 3 and 4B. Evidently, phosphorylated receptor opens spontaneously with higher probability P_o = 0.5% (Fig. 5A, Table 1). For comparison, the channel activity of unphosphorylated receptor activated by 1 μM ACh is displayed in Fig. 4C. At this ACh concentration, the frequency of opening is substantial and the extent of desensitization is relatively modest; P_o = 14% (Fig. 5A, Table 1). Corresponding high-resolution single-channel current recordings for the three experimental conditions are illustrated in the lower panels of Fig. 4. γ is not altered by phosphorylation: in symmetric 0.5 M KCl γ is 44, 47, and 45 pS, for unphosphorylated AChR, kinase-activated AChR, respectively (Table 1). Phosphorylated AChRs exhibit, in addition, a substate (γ =18 ± 4 pS, N=4), with a frequency of occurrence of <20%. Whereas the spontaneous activity of unphosphorylated AChR (Fig. 4A) is dominated by isolated brief events, the pattern of kinase A-activated AChR (Fig. 4B) resembles that of ACh-activated receptors (Fig. 4C) in that the frequency of events is higher and openings tend to appear isolated or in groups of two to four successive events. Thus, unliganded, phosphorylated AChRs exhibit channel activity comparable to that of unphosphorylated, ACh-activated AChRs. Similarly, this effect is sensitive to BGT in a concentration dependent manner; at 200 nM toxin, the open probability is practically undetectable (Fig. 5A).

Single-channel activity of unliganded, phosphorylated AChRs is similar to that of ACh-activated (unphosphorylated) AChRs. The similarity between the single-channel activity of unliganded, phosphorylated AChRs and ACh-activated (unphosphorylated) AChRs is further

underscored by the modification of the channel kinetic parameters reflected in the magnitude of open and closed channel lifetimes (Table 1). Computation of open lifetime distributions indicates that, similar to the unphosphorylated AChR (4-7,45), the kinase A-activated AChR has two kinetically distinct open states, short- and long-lived. The frequency of occurrence of long opening events (Fig. 5D) and the magnitude of both time constants (Fig. 5B and C) increase after phosphorylation, as they do with agonist concentration (4-7). Phosphorylation, therefore, is correlated with an increased probability of occurrence of the long-lived open state (Fig. 5D).

To rigorously assess the validity of the results, multiple records of unmodified and phosphorylated AChRs were subjected to statistical analysis of significance using the Mann-Whitney rank sum test (46). In view of the stochastic nature of the process – i.e., single events of low frequency and random occurrence – and the variable density of AChRs per membrane (4,44,45), data were collected over long recording periods. Results of the analysis are summarized in Table 1. At a stoichiometry of 0.3 mol of phosphate per mol of AChR the probability of channel opening in absence of ACh is > 6-fold, higher than that of unmodified AChRs; the difference is very significant ($P< 0.0002$). The increased open probability arises primarily from an increased occurrence of the long-lived open state (A_{OL}) and a concurrent prolongation of its lifetime (τ_{OL}). The > 3-fold lengthening of τ_{OL} and the increment of A_L/A_S are very significant ($P< 0.007$ and $P< 0.02$, respectively). Values from experiments at low phosphorylation stoichiometries (0.3 mol of phosphate per mol of AChR) are calculated from records exhibiting channel activity of both phosphorylated and unmodified AChR populations. Accordingly, increasing the extent of phosphorylation should exacerbate the effect on P_o and on the other channel kinetic parameters. Indeed, as shown in Table 1 and Fig. 5, at a stoichiometry of 1 mol phosphate/mol AChR, there is an increment of ~ 40-fold in the opening frequency with $P_o = 3\%$ and a concurrent increased probability of occurrence of the long-lived open state. At this stoichiometry, the extent of channel activation by kinase emulates that evoked by ACh in the 10^{-7} M concentration range. Hence, the extent of channel activation by protein kinase A is correlated with that of AChR phosphorylation.

Protein phosphorylation may be considered as an intracellular ligand which may act synergistically with cholinergic ligands to modulate receptor sensitivity for its ligand. Phosphorylation of AChRs by protein kinase A was reported to increase the rate of desensitization (12). This conclusion was inferred from fast-flux measurements obtained during the initial 12 ms after activation of AChRs preincubated (10 μM) and activated (50 μM) with desensitizing concentrations of ACh. By contrast, protein kinase A phosphorylation increases the AChR channel opening probability as determined from single-channel measurements over recording periods of several minutes in the presence of low ACh concentrations (1 μM) at which AChR desensitization is low (19) or, as reported here, in the absence of agonist to minimize the occurrence of desensitization. Taken together, these observations imply that phosphorylation may act synergistically with cholinergic ligands to modulate the sensitivity of the receptor to its ligand, thereby increasing the channel open probability and the rate of receptor desensitization.

This modulatory mechanism may exert differential efficacy depending on which AChR subunit is preferentially phosphorylated. Protein kinase A primarily phosphorylates the γ and δ subunits at distinct serine residues considered to be located in the cytoplasmic loop connecting the postulated third and fourth transmembrane segments (13,9,47). Furthermore, there are two potential phosphorylation sites in the δ subunit that are differentially phosphorylated in response to distinct stimuli applied to muscle cells (15). Accordingly, it is plausible that the functional response of the receptor depends on the specific phosphorylation site that is covalently modified. There is precedent for such a dual regulation by serine/threonine-specific protein kinases, whereby receptor activity can be activated or inactivated by phosphorylation depending on which

phosphorylation site is the target (for review see 48). In addition, AChRs are substrates for several protein kinases including protein kinases A (11-13) and C (14), tyrosine-specific kinase (16,17) and a calcium/calmodulin-dependent kinase (15). Thus, this differential regulatory mechanism may be additive.

The key finding that AChRs are activated by protein kinase A catalyzed protein phosphorylation independently of a binding reaction at the natural ligand recognition site is compatible with the notion that protein phosphorylation effectively acts as an intracellular ligand and that the phosphorylation sites may be considered as cytoplasmic ligand binding sites. That receptor proteins may be activated or inactivated by addition or removal of phosphate in the absence of extracellular cues suggests that this may have important implications for signal transduction pathways which consider receptor phosphorylation/dephosphorylation events critical in cell signaling and transformation (49).

Protein serine phosphorylation of AChRs by kinase A increases the probability of channel opening independent of ACh concentration. To correlate the extent of protein phosphorylation with the modifications of the AChR channel properties, samples of AChRs were prepared under conditions equivalent to those determined to produce specific levels of phosphorylation (Fig.3) and, after phosphorylation, incorporated into planar lipid bilayers for assay. The results of a series of experiments conducted in 0.5 M KCl, activated at 0.5μM ACh and recorded at V=100 mV are illustrated in Fig. 6. The top family of single-channel records (Fig. 6A) are from the control preparation. The single-channel conductance, γ, is 47 pS and it is calculated from the experimental histograms, which are fitted with the sum of two Gaussian distributions for the closed- and open-channel current levels (23) as illustrated in Fig. 6. Histograms of 15 sec segments of the recordings in which only one channel was open at any given time were analyzed. The relative frequency of occurrence of each state is determined from the area under the Gaussian distribution curve. The probability of the channel open state is 4%. As shown in Fig. 6B at stoichiometries of 0.3 mol phosphate per mol AChR, P_O increases to 16% whereas γ is practically unaffected (46 pS). At higher stoichiometries of phosphorylation the modification is more dramatic, as displayed in Fig. 6C: P_O increases ~90% at stoichiometries of 1.0 mol phophate/mol AChR; γ, however, remains virtually unaltered (45 pS). Equivalent results were obtained in 0.5 M NaCl, with the exception that γ=39-42 pS, in agreement with the known relative selectivity between K^+ and Na^+ of 1.2 (4).

The results of eight different experiments analyzed as described in Fig. 6 are summarized in Fig. 7. Clearly, the probability of channel opening increases with the stoichiometry of phosphorylation of the AChR. It is worth noting that at 0.99 total phosphate incorporated per mol of AChR the relative phosphorylation of individual subunits is approximately 0.05, 0.11, 0.39 and 0.44 for α, β, γ, and δ subunits, respectively (Fig. 3).

The dependence of the probability of AChR channel opening on ACh concentration was studied at different phosphorylation stoichiometries in both 0.5 M KCl and NaCl. Equivalent results have been obtained in KCl and NaCl. The results of the analysis obtained in KCl at a stoichiometry of 1.0 mol phosphate/mol AChR are summarized in Fig. 8. For the unphosphorylated AChR, the frequency of channel openings in absence of ACh is extremely low (P_o < 1%). P_O increases with ACh concentration from approximately 5% at 0.5 μM to approximately 25% at 5 μM ACh. Phosphorylation dramatically increases the AChR open probability at all ACh concentrations tested. For example, at 0.5 μM, P_O increases from approximately 5% to > 90% after phosphorylation. A plausible interpretation of this result is that phosphorylation increased the sensitivity of the receptor for its ligand. This notion is further supported by the fact that, even in the absence of ACh, the frequency of channel openings is

significantly increased approaching P_o values of up to 5% at total phosphorylation stoichiometries of approximately 1 mol phosphate per mol AChR.

AChR channel activity is modulated by protein tyrosine kinase and phosphatase. Fig. 9 illustrates single-channel currents recorded from lipid bilayers containing purified AChR activated by 1 μM ACh. Recordings obtained before and after the addition of tyrosine specific protein kinase, PTK, and/or phosphatase, PTP, are displayed. The experimental protocol allows the functional selection of a single population of AChR by restricting ACh to the compartment inside the recording pipet with the simultaneous enzyme treatment performed in the external bath solution (18). AChR channel activity is characterized by the paroxysmal occurrence of events at relatively high frequency, separated by quiescent periods reflecting a modest onset of desensitization (Fig. 9A and 9B, left panels). The sections indicated by arrows are displayed below at higher resolution. Note that discrete events with single-channel conductance of 44 pS (symmetric 0.5 M KCl) and short (≤ 1 ms) and long (≥ 5 ms) open times are readily resolved. Addition of PTK (20 U/ml) to the bath increased AChR channel activity (Fig. 9A, middle panel). The increment in AChR channel activity arises from an increase in the frequency of events and a prolongation of the channel open lifetimes, as clearly discerned in the recordings displayed at high resolution. Subsequent addition of 12 mM EGTA, to arrest PTK activity, and PTP (5 U/ml) reversed the activating effect of the tyrosine kinase, and further depressed the AChR channel activity beyond that prevalent in the control record (Fig. 9A, right panel). The single-channel conductance was 45 and 43 pS for PTK and PTP treated AChR, respectively. Modifications of AChR channel activity by both enzymes is also reversible when the enzyme first added is PTP as shown in Fig. 9B. AChR channel activity sharply decreased after addition of PTP (Fig. 9B, middle panel), but was notably augmented upon addition of PTK (Fig. 9B, right panel).

Modifications of AChR channel activity correlate with the extent of protein tyrosine phosphorylation. Protein-tyrosine phosphorylation is the underlying modification that produces the changes in AChR channel activity, as indicated by the phosphotyrosine detection pattern shown in Fig. 10A. Western blot analysis using monoclonal antibodies against phosphotyrosine shows that AChR is endogenously phosphorylated in tyrosines (3,17; Lane 1). The extent of AChR phosphotyrosine in the β, γ and δ subunits decrease or increase upon the action of PTP or PTK, respectively (Lanes 2 and 3); PTK action is reversed by subsequent treatment with PTP (Lane 4). No change in the extent of AChR phosphotyrosine was detected when ATP, kinase, or β-mercaptoethanol were omitted from the reaction mixture. Clearly, modifications of AChR channel activity described in Fig. 9 correlate with the extent of AChR tyrosine phosphorylation. No change in signal was detected when AChR was phosphorylated by protein kinase A or C (Lanes 5 and 6), known to phosphorylate serine residues, confirming the specificity of the imunoassay. Fig. 10B illustrates the time course of ^{32}P incorporation into AChRs. Unmodified AChRs, which are endogenously phosphorylated to some extent (Fig. 10A, Lane 1), incorporate an additional 1.02 ± 0.06 mol ^{32}P/mol AChR, whereas receptors, dephosphorylated by the action of PTP, incorporate up to 2.2 ± 0.1mol ^{32}P/mol AChR after PTK treatment. This indicates that both PTK and PTP acted on unmodified AChRs by adding or removing the same amount of phosphate. Phosphate incorporation occurs in a time scale comparable to that within which the changes in AChR channel activity are measured (Fig. 9 and Fig. 11B). Thus, protein-tyrosine phosphorylation and dephosphorylation modulate AChR channel activity.

AChR channel gating is regulated by the interplay of ACh concentration and tyrosine phosphorylation. To examine the mechanism of channel modulation by protein phosphorylation, channel activity of dephosphorylated, unmodified and phosphorylated AChRs

was characterized as a function of ACh concentration. In absence of ACh, the receptor channel opens spontaneously but infrequently, with a probability of opening of ≤ 0.1% (18,45). Phosphorylation by kinase A increases AChR channel activity in absence of ligand (18). By contrast, unmodified and tyrosine phosphorylated AChRs display similar channel activity. This fact underscores the notion of differential modulation of AChR channel activity by distinct phosphorylation sites, since phosphate incorporation by kinase A occurs on serine residues in the γ and δ subunits (11-13).

Fig. 11A shows the AChR channel activity, elicited at three different ACh concentrations, as a function of the extent of receptor tyrosine phosphorylation. At 0.1 and 1 μM ACh, unmodified AChRs exhibit channel activity characterized by occurrence of relatively frequent and brief events (middle panels). At these ACh concentrations, phosphorylated AChRs show a significant increase of the frequency of channel opening and a prolongation of channel open lifetime (right hand panels). Conversely, dephosphorylated AChRs display a decrease in channel activity. The records are characterized by the presence of sporadic and brief events, separated by long quiescent periods (left hand panels). The time course of change in the channel open probability, P_O, is depicted in Fig. 11B. Unmodified AChRs displayed a steady-state P_O = 0.04 and 0.11 when activated by 0.1 and 1 μM ACh, respectively. Phosphorylation of AChRs promotes a rapid increase of P_o to a steady state value that fluctuates around 0.75 during the recording period (12 min), whereas AChR dephosphorylation reduced P_O by a factor ≥ 7.

In contrast, an opposite effect was observed when receptor channel activity was elicited by 10 μM ACh. Notably, phosphorylation of AChRs resulted in a decline of receptor channel activity as compared with unmodified receptors (Fig. 11A, middle and right hand panels); from P_o = 0.2 for unmodified AChRs to P_O = 0.003 for phosphorylated AChRs (Fig. 3B, bottom panel). Given the reversibility of the phosphorylation effects (Figs. 9,10), dephosphorylated AChR should display an increment of channel activity when assayed at 10 μM ACh. In fact, dephosphorylated AChRs show a 4-fold higher P_O than unmodified receptors as illustrated in Fig. 11A, (middle and left hand panels) and Fig. 11B. Channel gating of dephosphorylated AChRs activated by 10 μM ACh resembles that exhibited by phosphorylated AChRs activated by either 0.1 μM or 1.0 μM of ACh.

Together, these results establish that regulation of AChR channel gating depends on a tight interplay between two distant structural domains of the protein, namely the ACh ligand binding site exposed to the extracellular surface of the AChR and the phosphorylation domain confined to the cytosol.

Tyrosine phosphorylation of AChR modulates the probability of channel opening. To rigorously assess the modulation of AChR channel activity by both phosphorylation state and ligand binding, dose-response analysis for phosphorylated, unmodified, and dephosphorylated AChRs was performed. As shown in Fig. 12A, phosphorylated AChRs display the greatest sensitivity to ACh and, therefore, activate and desensitize at lower agonist concentrations than those required for unmodified and dephosphorylated receptors. Modulation of AChR channel gating by tyrosine-specific phosphorylation was further examined by analysis of channel open lifetimes (Fig. 12B, C). Open lifetime distributions are well fitted by the sum of two exponentials consistent with the occurrence of two kinetically distinct open states, short(S)- and long(L)-lived (5-7). For unmodified AChRs, the time constants for the short and long open states are not affected by the agonist concentration (Fig. 12B). The frequency of occurrence of the long events over the short (A_L/A_S) increases with ACh concentration. At high ACh (100 μM), however, a decrease in the A_L/A_S ratio is observed, reflecting that AChRs are preferentially in the desensitized state (Fig. 12C). By contrast, for phosphorylated and dephosphorylated receptors both parameters (τ_{OL}, A_L/A_S) increase with agonist concentration, except for 100 μM ACh at

which concentration, as in unmodified AChRs, a decrease is observed (Fig. 12B, C). Note that changes in long open time and A_L/A_S ratio follow a similar pattern to that exhibited by the open probability (Fig. 12A). Hence, the increased open probability of the activated AChR channel is accounted for by the predominant occurrence of the long-lived open state and the concomitant lengthening of its lifetime.

Dual regulation of receptor function. A consequence of two interacting mechanisms operating on a single receptor is that tyrosine phosphorylation regulates receptor sensitivity. We define AChR sensitivity as its propensity to undergo a functional change in response to agonist binding: AChRs with increased sensitivity would respond at lower agonist concentration. In our measurements, the observable is channel opening. Therefore, to simplify the analysis, dose-response plots of the open probability for phosphorylated (H), unmodified (M) and dephosphorylated (L) AChRs, summarized in Fig. 12A, were normalized and compared with theoretical dose-response curves for three ligands with high (H), medium (M) and low (L) affinities, as shown in Fig. 13A and B. Dose-response curves are calculated for the reaction scheme: $R \overset{K_{L/2}}{\leftrightarrow} RL \overset{2K_L}{\leftrightarrow} RL2 \rightarrow$ function, where R denotes receptor, L, the ligand and function is channel opening, which our experiments measure. We interpret the attenuation of the experimental data displayed in Fig. 13A at higher agonist concentrations as a reflection of desensitization, whereas the calculated curves shown in Fig. 13B ignore it. The above discussion explicitly describes affinity in a functional context, namely, the ability to elicit a response (50): a high affinity agonist evokes a response at a lower concentration than a low affinity ligand. Concomitantly, the evoked response inactivates at lower concentrations of the former than of the latter. Note that tyrosine phosphorylated AChRs are characterized by an open probability curve for ACh equivalent to that corresponding to a ligand with high affinity for the receptor. Conversely, dephosphorylated receptors display a dose-response curve characteristic of a low affinity agonist (51). It follows, then, that the extent of receptor phosphorylation effectively shifts the dose-response relationship for a single agonist to lower concentrations. The magnitude of the shift parallels the degree of phosphorylation with a relative AChR sensitivity to ACh that is greatest for phosphorylated AChR and decreases progressively with dephosphorylation (Fig. 13A,B). The sensitivity of receptor response to ACh is affected to different relative extents depending upon the relative values of protein phosphorylation with the greatest change occurring from virtually phosphorylated to dephosphorylated states. When we consider desensitization within the context of this simplified model, it can be shown by using computer simulations (52), that the agonist concentration dependence for inactivation of the AChR response is also shifted to the left with the greatest change occurring for phosphorylated AChRs. Thus, receptor tyrosine phosphorylation correlates with an increment of AChR sensitivity to its agonist.

Protein kinase C phosphorylates AChR δ subunit. The activity of protein kinase C results in the preferential phosphorylation of the AChR δ subunit, as shown in Fig. 14. For illustration purposes the protein phosphorylation pattern produced by protein kinase A is presented in the first three lanes. It is clear that AChR phosphorylation by kinase A modifies primarily γ and δ subunits whereas the δ subunit is the only substrate of protein kinase C, under otherwise equivalent experimental conditions. The serine residue recognized by protein kinase C is different from those modified by protein kinase A, as inferred from cross-phosphorylation experiments in which AChR was initially phosphorylated with non-radioactive ATP by either kinase A or C and then phosphorylated in presence of [γ-^{32}P]ATP by the other kinase. The results show that the serine residues modified by kinase A or kinase C are different because prephosphorylation by one kinase did not prevent phosphorylation by the second, independent of

the order in which the prephosphorylation reaction proceeded. The efficacy of phosphorylation in this experimental protocol for the two protein kinases results in phosphorylation stoichiometries of 0.83 ± 0.18 mol phosphate/mol AChR (n=3) and 0.17 ± 0.06 mol phosphate/mol AChR (n=3) for protein kinase A and C, determined under identical conditions. As a control, when prephosphorylation and phosphorylation reactions were performed with the same kinase, the additional incorporation of ^{32}P to AChR subunits was negligible.

Protein serine phosphorylation of AChRs δ subunits by protein kinase C is sufficient to increase the probability of channel opening. As illustrated in Fig. 15A, the frequency of spontaneous openings in absence of ACh is low and the openings are very brief. After addition of protein kinase C and ATP, a significant augmentation in the frequency of occurrences and a prolongation of their open time occurrs, as discerned in the lower traces, which display at higher resolution the sections of the records indicated by the arrows. The results of comparable experiments for AChRs activated by 1μM ACh are illustrated in Fig. 15B. The frequency of openings is significantly higher than the spontaneous activity displayed in Fig. 15A, yet it is still moderate. Addition of protein kinase C and ATP leads to a marked increment in the frequency of occurrences and a concomitant lenghtening of the open time, as disclosed in the high resolution records. The single-channel conductance was not modified by the activity of protein kinase C. Thus, phosphorylation of AChRs δ subunits is sufficient to increase the open-channel probability.

Protein kinase C phosphorylated AChR exhibits an increased open-channel probability as a function of ACh concentration. As shown in Fig. 15, protein kinase C leads to activation of AChRs both in the absence and presence of ACh. To systematically assess the interplay between ACh binding and protein phosphorylation, single-channel recordings of unmodified and phosphorylated preparations were collected and the probability of channel opening was studied in the absence of ACh, at different ACh concentrations, and at three different extents of protein phosphorylation, namely, 0.1, 0.5, and 1.0 mol phosphate/mol AChR. The data processed to this date involve those obtained at a stoichiometry of 0.1 mol phosphate/mol AChR, and the numbers reported in Fig. 16 are means of at least three different experiments in each condition, with SEM<10%. In absence of ACh, the spontaneous activity is characterized by the infrequent occurrence of very short openings, with a $P_o < 0.001$. Phosphorylation by protein kinase C increased the frequency of openings and consequently P_o to values approaching 0.15. At 1 μM ACh, protein phosphorylation promoted a drastic activation of the channel arising from an increment in the frequency of openings and a prolongation of channel open lifetime. P_o of unmodified AChRs was 0.1 and increased to 0.5 after phosphorylation. The increased open probability arises primarily from an increased occurrence of the long-lived open state and a concurrent prolongation of its lifetime, as previously described for AChRs phosphorylated by protein kinase A (Fig. 8). In contrast, at 10 μM ACh the effect of protein kinase C is modest. This result should be contrasted with the drastic modification evoked by protein-tyrosine phosphorylation at 10 μM (Fig. 12) in which P_o was sharply attenuated. The single-channel conductance of unmodified and protein kinase C phosphorylated AChRs was equivalent. Single-channel recordings have been collected at 0.05, and 5 μM ACh and are currently being processed. It is anticipated that the analysis will be complete in the next few weeks and will provide information conducive to formulate a comprehensive scheme for the regulation of AChR by protein phosphorylation involving the selective modification of distinct residues (serine/threonine or tyrosine) in different AChR subunits arising from the substrate specificity of the protein kinases and phosphatases described in this and previous reports.

Differential modulation of AChR open-channel probability by selective phosphorylation of distinct residues in specific subunits. Phosphorylation of AChRs by distinct protein kinases modulates the channel activity in a diverse way. The common consequence of AChR phosphorylation is an increase in the open-channel probability. The diversity of effects occur when the interaction with the ligand-binding motif enters into play. Accordingly, protein-tyrosine phosphorylation does not activate the AChRs in absence of ligand but it produces the most drastic increment in the sensitivity of AChR for ACh, leading to an apparent shift of the dose-response curve to lower agonist concentrations. In contrast, protein-serine phosphorylation by both protein kinase A and C activate AChRs in the absence of ACh and increase open-channel probability in its presence, but whereas the increment produced by kinase A is featured at all ACh concentrations tested, modulation by kinase C is more apparent at ACh $\leq 1\mu M$. It is plausible that *in vivo* phosphorylation by the distinct kinases and dephosphorylation by different phosphatases occurs on different subunits and to different extents, thereby conferring a response diversity to the synaptic terminal.

Phosphorylation of AChRs in human cerebellar medulloblastoma cells. The effects of protein phosphorylation on AChRs in intact nerve cells were investigated in the human cerebellar medulloblastoma cell line TE671 (41,42) by patch clamp recording techniques (36). As previously documented in the Midterm report, this cell line expresses AChRs that are blocked by α-BGT. To assess the effect of protein kinases on the rate of AChR desensitization purified catalytic subunit of protein kinase A (10 μg/ml) and ATP (1mM) were included in the solution filling the recording pipet and the amplitude and kinetics of the current recorded 1 min after accessing the cell was recorded at periodic intervals. No significant changes were recorded under these conditions. Similar results were obtained by Siara, et. al. (53).

No significant modification of either the amplitude or the kinetics of the ACh-activated currents was detected if recombinant PTK ($p43^{V\text{-}abl}$ from Oncogene Science, Manhasset, N.Y.) was used (2 units/ml dissolved in 0.1% PBS, phosphate buffer) instead of catalytic subunit of protein kinase A.

To assess the effect of protein kinase C on the AChR we used a lipid soluble phorbol ester (12-O-tetradecanoyl-phorbol-13-acetate, TPA, Sigma) known to penetrate cell membranes and activate intracellular protein kinase C (54). We used the cell-attached configuration to obtain single-channel recordings. The solution inside the recording pipet was adjusted to mimic the intracellular composition aiming to obtain recordings under symmetric ionic solutions; it contained (in mM): KCl 140, NaCl 5, TES 5, glucose 10, $MgCl_2$ 4, pH adjusted to 7.4. The ACh concentration was 0.5 μM. As described in the Midterm report, TPA reduced the number of open channels. The effects of TPA were not consistent from cell to cell. TPA is known to produce non-specific effects of ionic currents recorded from cellular preparations.

The publication of Siara, et.al., (53) reporting results equivalent to those obtained by our group and the modest or nonspecific effects obtained with PTK and protein kinase C, respectively, led us to discontinue this facet of the program (Midterm Report).

Electrophysiological characterization of the subunit specific mutants of the *Torpedo* AChR expressed in *Xenopus* oocytes. Deletion mutants were produced from the *Torpedo* β, γ and δ subunit cDNAs for the presumed cytoplasmic domains that contain the phosphorylation sites for protein kinase A and the tyrosine kinase. This cytoplasmic loop encompasses a segment extending from the carboxy-terminus of the presumed M3 segment to the amino-terminus of the putative M4 segment. For kinase A, the peptide segments deleted were amino acid (AA) 353-371 for the γ subunit (nucleotides deleted 1228-1285), and AA 360-379 for the δ subunit (nucleotides deleted 1598-1657). For the tyrosine kinase phosphorylation site the tyrosine in position 355 of

the β subunit was replaced by a phenylalanine (DNA change A1179->T). Deletions were confirmed by DNA sequencing. cDNAs were transcribed *in vitro* and mRNA was prepared for the wild-type subunits as well as for the mutants. mRNAs were injected into *Xenopus* oocytes. Injection of wild-type mRNAs for the four subunits resulted in the expression of functional AChRs. The amount of AChRs expressed on the surface of the oocyte was determined by the specific labeling with ^{125}I labeled α-BGT [Midterm Report].

The electrophysiological characterization of the *Torpedo* AChRs expressed in *Xenopus* oocytes after injection of AChR subunit specific cRNAs was pursued. Macroscopic currents were recorded using the two electrode voltage clamp. Currents were evoked by bath addition of ACh. The current response is a transient that rises to a peak and desensitizes following an exponential time course. The peak amplitude was used as an assay of the extent of expression and the rate of desensitization as a functional parameter for comparisons between wild-type AChRs and the deletion mutants.

As summarized in Fig.17, the ACh-evoked current of AChRs containing the γδ deletion mutant is significantly lower than that of control AChRs or AChRs containing solely the γ or δ mutation. The Mann-Whitney rank sum indicates that the results are very significant with a $P \leq 0.001$ (N=8). The current values are given with respect to the control current response activated by 5 μM ACh (950 ± 456 nA, N=8). The number of α-BGT binding sites expressed on the surface of the oocytes is comparable (within the experimental error, i.e. 10%) in all indicated combinations. This indicates that AChRs containing the γδ double deletion mutant are less conductive or open more briefly than wild-type AChRs.

As summarized in Fig.18, the rate of desensitization ([ACh] = 50 μM) is considerably reduced in AChRs containing the γδ mutations, although a similar effect was obtained with the single γ deletion mutant whereas the single δ deletion mutant was comparable to wild-type AChR. The γ subunit appears to be a major component that determines the desensitization rates, as inferred from this assay and these mutants.

Significant variability was encountered in the experimental data depending on the preparation of injected cRNA for the distinct mutants, the survival of injected oocytes, the magnitude of the current responses of oocytes expressing the AChR mutants. The lack of internal consistency of the results led to suspect problems in RNA processing by the oocytes leading to defective assembly of the AChR complex. Similar erratic and variable responses have been observed by other research teams (55-57). It was, therefore, judged prudent to search for a simpler and reliable AChR to pursue our tasks. This was the rationale for the selection of neuronal AChR α7.

Point mutations of the putative phosphorylation site for kinases in the neuronal AChRα7 clone modify the channel properties of the gene product expressed in *Xenopus* oocytes. The AChRα7 clone encodes a cholinergic receptor. The gene product expressed in amphibian oocytes assembles into a homomeric complex that displays the characterisitics of a nicotinic cholinergic receptor channel. As shown in Fig. 19, application of ACh to the Ringer's solution bathing the oocytes evokes an inward transient current that rapidly desensitizes in the presence of agonist. The current amplitude increased with agonist concentration. Receptor activation and desensitization kinetics accelerated with agonist concentration (Fig. 19). Homomeric AChRα7s were highly sensitive to α-BGT: application of 100 nM toxin blocked the ACh elicited current by >90%.

The sequence of AChRα7 contains a consensus phosphorylation motif for kinase A. Serine 344 is a unique phosphorylation site (Fig. 20). In contrast, AChRs from neuromuscular junctions are heteromeric complexes composed of four different protein subunits (α,β,γ,δ) that contribute a total of nine potential phosphorylation sites. The phosphorylation motif is confined to a 22-amino acid stretch in the postulated cytoplasmic loop connecting the predicted transmembrane

segments M3 and M4. Such complex structure has represented a serious obstacle to gain molecular information on AChR functional regulation. Accordingly, we proceeded to introduce point mutations at the unique phosphorylation site of AChR7, namely S344. The following mutations were generated and the functional consequences investigated after expression of the respective cRNAs in *Xenopus* oocytes:

[1] S->A, to generate a non-modifiable AChR, presumably comparable to a dephosphorylated AChRα7, wild-type;
[2] S->E, and
[3] S->D, to introduce a negatively charged residue that may mimic the phosphorylated AChRα7 (58);
[4] S-> T,
[5] S-> Q, and
[6] S-> N, as negative controls for mutants [1], [2] and [3], respectively.

The results of the functional analysis, summarized in Fig. 21 and 22, suggest that the sensitivity of the AChR to its ligand is modulated by this site. The most drastic effect was displayed by the AChRα7S->E mutant which exhibits a dose-response curve shifted to higher agonists concentrations (Fig. 21) and a slower rate of receptor desensitization (Fig. 22). Significantly, the AChRα7S->Q mutant reversed these effects and featured properties comparable to those of the non-modifiable mutant [S->A] and the other control mutants [S->T] and [S->N]. These effects are modest but statistically significant.

Chimeric AChRa7 gene products implanted with the phosphorylation motif of the muscle-type AChR β, γ and δ subunits display modified electrophysiological properties in amphibian oocytes. The results of the electrophysiological analysis of the chimeric constructs are summarized in Fig. 23 and 24. AChRα7 and the deletion mutant express large amplitude currents elicited by ACh. The control chimera in which the deleted 22-amino acid segment was reinserted expressed lower amplitude current responses (about 2-fold). In contrast, the chimeric constructs implanted with the phosphorylation motif of the β and the δ subunits displayed significantly lower current responses at all ACh concentrations tested (Fig. 23). No significant changes in the rate of receptor desensitization were identified (Fig. 24). At present, no expression of the chimeric γ insert has been detected and the subcloning procedure is reexamined.

The combined results of site-directed mutagenesis and "cassette mutagenesis" indicate that phosphorylation is important for AChR action. The end results obtained from the oocyte expression system, inferred from macroscopic current resposes to ACh, contain contributions from several cellular processes involved in the processing of the message, insertion of the mature protein into the membrane, the stability of the product, and modifications of the intrinsic channel properties (permeation and gating). The story that is emerging from the recombinant strategy is, at present, fragmentary. Work in progress is directed to assess the number of receptors incorporated into the oocyte as determined from toxin-binding determinations. This information will assist in establishing if the lower levels of expression of the mutants arise from a reduced number of AChRs in the surface membrane or from alterations in the channel properties. Furthermore, mâcro-patch recordings from the same oocytes in which the macroscopic current recordings are obtained will provide information about the single-channel properties of the expressed mutants independently of other cellular factors and, therefore, assist in tracing the basis for the modified activity of the mutant AChR at the level of channel permeation or gating, as described for the reconstituted AChRs in lipid bilayers.

Studies on voltage-gated sodium channels. The rat brain II sodium channel cDNA clone was expressed in oocytes, as described in ref. 38, and the effects of pharmacological agents that modulate protein phosphorylation examined. As shown in Fig. 25A and 25B for the phorbol ester

TPA (12-0-tetradecanoyl-phorbol-13-acetate), an activator of protein kinase C, modifies the electrophysiological properties of the expressed channel. A family of sodium currents in response to a series of test potentials that ranged from -70 mV to 80 mV in increments of 10 mV, from a holding potential of -90 mV is illustrated in Fig. 25A. The typical transient time course of sodium currents is evident with a fast activation and slower inactivation. Addition of 1 μM TPA to the same oocyte progressively and drastically reduces the sodium current as illustrated in Fig. 25B; this record was taken 40 min after TPA addition and shows a 5-fold reduction in current amplitude. The effect was not reversible after perfusion for over one hour. By contrast, treatment of different oocytes with 100 μM 8-Br cyclic AMP and 100 μM IBMX (3-isobutyl-1-methyl xanthine) to activate cyclic AMP dependent protein kinase and inhibit cyclic AMP hydrolysis by the phosphodiesterase, shows no effect on the amplitude or the kinetics of the sodium channel current. This observation was confirmed by other research teams (59-64). The results suggest a specific regulation of sodium channels by a protein kinase C-activated pathway.

Molecular cloning and functional expression of a voltage-gated sodium channel from human brain. A cDNA library derived from human cerebral cortex was screened for the presence of sodium channel α subunit specific clones. Ligation of three overlapping clones generated a full length cDNA clone, HBA, that provided the complete nucleotide sequence coding for a protein of 2005 amino acids. The predicted structure suggests four homologous repeats and exhibits greatest homology and structural similarity to the rat brain sodium channel II (65).

Amino acid sequence alignments (66) and hydrophobicity plots reveal the presence of several canonical structural features predicted for other sodium channels (67,68). For HBA, the four internal homology repeats (I-IV) extend from amino acid 129 to 427, 759 to 985, 1208 to 1475, and 1531 to 1778. Within each homologous repeat, there are eight potential transmembrane segments with S4 (Sd) exhibiting the 3-fold repeat of basic residues (67,68).

The human brain and the cardiac or skeletal muscle channels differ in several amino acids, most of which occur in the loops connecting repeats I-II and II-III and do not change the assignment of potential glycosylation or phosphorylation sites postulated for other sodium channels (67,68). Potential glycosylation sites (69) occur at nine asparagine residues assigned to extracellular loops C-terminal to the S5 segments of homologous repeats I and III. Consensus patterns for cAMP-dependent protein kinase phosphorylation (70) are identified in eight stretches. Further, 14 potential sequences for protein kinase C phosphorylation (71) are recognized. It is significant that all presumed phosphorylation sites are predicted to be in the cytoplasmic domain of the protein (67,68). Acidic residues considered to contribute to the tetrodotoxin (TTX) binding site are conserved and assigned to the segment denoted as Sg (67) or SS2 (68): 384, 387, 942, 945, 1426, 1717. The HBA protein, thus, exhibits the structural features postulated for other sodium channels (9,67,68).

Transient Expression in Mammalian Cells. Electrophysiological properties of the sodium channel coded by the HBA DNA sequence were characterized after transfection in CHO cells (65). A family of sodium currents in response to a series of depolarizing voltage steps of 10 ms duration, from a holding potential of -100 mV, is illustrated in Fig. 26A. Currents increase to a peak and then decline. Kinetics of early activation are sigmoidal and of subsequent decay approximately exponential. A comparison of the amplitude and kinetics of the currents recorded at -20 and 0 mV show that both activation and current decay accelerate at progressively more depolarized potentials. The peak current-voltage (*I-V*) relationship is shown in Fig. 26B. Depolarization to voltages positive to -40 mV rapidly activate sodium currents. The peak current, I_{peak} (1332 ± 487 pA), recorded in 18 different cells was obtained at test potentials of 5.6 ± 8.6

mV (mean ± SD). In contrast, control CHO cells transfected with vector devoid of HBA cDNA insert express an endogenous sodium channel with I_{peak} = 201 ± 138 pA (N = 10) at V = 18.8 ± 6.4 mV. The peak sodium conductance g_{peak} increased with depolarizing voltages to a maximum at V ~20 mV, exhibiting a half-activation voltage at V = -24 mV and an e-fold change in g_{peak}/8.3 mV (Fig. 26C). The Hodgkin-Huxley (72) inactivation parameter (h_∞) indicates that at V = -34 mV half of the sodium currents were inactivated (Fig. 26D). Sodium currents were blocked by 100 nM TTX (Sigma Chemicals). Blocking was partially reversible, the currents recovering up to 70% of control.

Overall, the HBA gene product displays macroscopic sodium currents that resemble the transient time course, kinetics, selectivity and TTX-sensitivity characteristic of sodium channels recorded in a variety of cells (73) including the human cerebellar medulloblastoma cell line TE671 (42).

3. Conclusions

A combination of strategies encompassing biochemistry, biophysics, molecular biology and pharmacology was implemented to converge on the question of the fundamental events in the regulation of cholinergic receptor channels by protein phosphorylation. The most significant finding of this program is that receptor function has a dual regulation by extracellular ligand binding and intracellular phosphorylation: AChRs are activated in absence of ACh by seryl-protein phosphorylation and both seryl- and tyrosyl-protein phosphorylation correlate with an increment of AChR sensitivity to its agonist. These results suggest that phosphate incorporation or removal from target receptors may be a critical metabolic cue in signal transduction. Protein phosphorylation, therefore, could generate a diversity of synaptic modifications dependent on the magnitude, time course and targeted residue of the phosphorylation reaction and, in turn, the efficacy of such regulation would be modulated by the concerted interplay with ligand binding. Phosphorylation of neurotransmitter receptors may, therefore, represent a fundamental means to optimize both initiation and termination of transmitter response that may have important implications for synaptic plasticity.

An important outcome of this program was the demonstration that protein phosphorylation is a critical signal for the assembly and stability of the AChR in the cell membrane. Mutational analysis conducted on both the muscle-type AChR from *Torpedo californica* and the neuronal AChRα7 demonstrated that the protein domain presumably involved in the phosphorylation events is also crucial for the insertion and assembly of AChR subunits into a functional entity in the cell membrane.

The concepts that emerged from this analysis were extended to members of the superfamily of voltage-gated channels, specifically sodium channels. A milestone in this program was the first isolation of a cDNA clone for a human brain sodium channel and the biophysical and pharmacological characterization of its gene product after its expression in mammalian cells. The availability of cDNA clones for human brain sodium channels and their expression in heterologous systems should provide a powerful system for a detailed investigation of the pharmacological properties of human brain proteins and, in combination with molecular modeling of the pore-forming structure, may provide insights towards the development of site-directed drug design.

4. References

1. Nestler, E.J. & Greengard, P. (1984) *Protein Phosphorylation in the Nervous System.* (Wiley, New York).
2. Hemmings, H.C., Narin, A.C., McGuinness, T.L., Huganir, R.L. & Greengard, P. (1989) *FASEB J.* 3, 1583-1592.
3. Swope, S.L., Moss, S.J., Blackstone, C.D. & Huganir, R.L. (1992) *FASEB J.* 6, 2514-2523.
4. Labarca, P., Lindstrom, J. & Montal, M. (1984) *J. Gen. Physiol.* 83, 473-496.
5. Labarca, P., Lindstrom, J. & Montal, M. (1984) *J. Neurosci.* 4, 502-507.
6. Labarca, P., Montal, M.S., Lindstrom, J. & Montal, M. (1985) *J. Neurosci.* 5, 3409-3413.
7. Labarca, P., Rice, J.A., Fredkin, D.R. & Montal, M. (1985) *Biophys. J.* 47, 469-478.
8. Montal, M., Anholt, R. & Labarca, P. (1986) *In: Ion Channel Reconstitution.*, ed. C. Miller (Plenum Press, New York and London), pp. 157-273.
9. Numa, S. (1989) *Harvey Lect.* 83, 121-165.
10. Galzi, J.-L., Revah, F., Bessis, A. & Changeux, J.-P. (1991) *Annu. Rev. Pharmacol.* **31**, 37-72.
11. Huganir, R. L. & Greengard, P. (1983) *Proc. Natl. Acad. Sci. USA* **80,** 1130-1134.
12. Huganir, R.L., Delcour, A.H., Greengard, P. & Hess, G.P. (1986) *Nature (London)* **321,** 774-777.
13. Yee, G.H. & Huganir, R.L. (1987) *J. Biol. Chem.* **262,** 16748-16753.
14. Safran, A., Provenzano, C., Sagi-Eisenberg, R. & Fuchs, S. (1990) *Biochemistry* **29,** 6730-6734.
15. Smith, M.M., Merlie, J.P. & Lawrence, J.C. (1989) *J. Biol. Chem.* **264,** 12813-12819.
16. Huganir, R. L., Miles, K. & Greengard, P. (1984) *Proc. Natl. Acad. Sci. USA* **8,** 6968-6972
17. Hopfield, J.F., Tank, D.W., Greengard, P. & Huganir, R.L. (1988) *Nature (London)* **336,** 677-680.
18. Ferrer-Montiel, A.V., Montal, M.S., Díaz-Muñoz, M. & Montal, M. (1991) *Proc. Natl. Acad. Sci. USA* **88,** 10213-10217.
19. Montal, M.S. & Montal, M. (1987) *Soc. Neurosci.* **13,** 798.
20. Shoepfer R, Conroy, W.G., Whiting, P. Gore M. & Lindstrom J. (1990). *Neuron* **5,** 35-48.
21. Couturier, S., Bertrand, D., Matter, J.-M., Hernandex, M.C., Bertrand, S., Millar, N., Valera, S., Barkas, T. & Ballivet, M. (1990) *Neuron* **5,** 847-850.
22. Suarez-Isla, B.A., Wan., K., Lindstrom. J. & Montal, M. (1983) *Biochemistry* **22,** 2319-2323.
23. Keller, B.U., Hartshorne, R.P., Talvenheimo, J.A., Catterall, W.A. & Montal, M. (1986) *J. Gen. Physiol.* **88,** 1-23.
24. Slice, L.W. & Taylor, S.S. (1989) *J. Biol. Chem.* **264,** 20940-20946.
25. Laemmli, U. K. (1970) *Nature (London)* **227,** 680-685.
26. Tonks, N.K., Diltz, C.D. & Fischer, E.H. (1990) *J. Biol. Chem.* **265,** 10674-10680.
27. Kyhse-Andersen, J. (1984) *J. Biochem. Biophys. Methods* **10,** 203-209.
28. Kunkel, T.A. 1985. *Proc. Natl. Acad. Sci. USA. 82:* 488-492.
29. Sanger,F., Nicklin, S. & Coulson, A.R. (1977) *Proc. Natl. Acad. Sci. USA.* **74,** 5473-5467.
30. Devereux, J., Haeberli, P. & Smithies, O. (1984) *Nucleic Acids Res.* **12,** 387-35.
31. Sambrook, J., Fritsch, E.F. & Maniatis, T. (1989) In: Molecular Cloning: A Laboratory Manual. 2nd Ed. Cold Spring Harbor Laboratory Press, Inc., N.Y.
32. Krieg, P.A., & Melton, D.A. 1984. *Nucleic Acid. Res.* **12,** 7057-7070.
33. Kinarska, M.M., Padgett, R.A. & Sharp, P.A. 1984. *Cell* **38,** 731-736.
34. Gundersen, C.B., Miledi, R. & Parker, I. (1983) *Proc. R. Soc.* London B **220,** 131-140.
35. Claudio, T., Paulson, H.L., Hartman, D., Sine, S. & Sigworth, F.J. (1988) *In: Current Topics in Membrane and Transport,* Vol 33, pp. 220-247.
36. Sakmann, B. & Neher, E. (1983) *Single-Channel Recording,* (Plenum Press, NY), pp 503.
37. Methfessel, C., Witzemann, V, Takahashi, T., Mishina, M., Numa, S. & Sakmann, B. (1986) *Pflügers Arch.* **407,** 577-588.
38. Sun W., Ferrer-Montiel A.V, Shinder, A.F., McPherson, J.P., Evans, G.A. & Montal M. (1992). *Proc. Natl. Acad. Sci. USA.* **89,** 1443-1447.
39. White, M.M. & Aylwin M. (1990) *Mol .Pharmacol.* **37,** *720-724.*

40. Tomaselli, G.F., McLaughlin, J.T., Jurman, M.E. Hawrot, E. & Yellen G. (1991) *Biophys J.* **60**, 721-727.
41. Luther, M.A., Schoepfer, R., Whiting, P., Casey, B., Blatt, Y., Montal, M.S., Montal, M. & Lindstrom, J. (1989) *J. Neurosci.* **9**, 1082-1096.
42. Gambale, F. & Montal, M. (1989) *Mol. Brain Res.* **7**, 123-129.
43. Carbonne, E. & Lux, H.D. (1987) *J. Physiol. (London)* **386**, 547-570.
44. Jackson, M.B. (1984) *Proc. Natl. Acad. Sci. USA* **81**, 3901-3904.
45. Jackson, M.B. (1986) *Biophys. J.* **49**, 663-672.
46. Colquhoun, D. (1971) *In: Lectures on Biostatistics. An Introduction to Statistics with applications in Biology and Medicine*, (Clarendon Press, Oxford), pp. 137-170.
47. Shroeder, W., Meyer, H.E., Buchner, K., Bayer, H. & Hucho, F. (1991) *Biochemistry* **30**, 3583-3588.
48. Dent. P., Lavoinee, A., Nakielny, S., Caudwell, F.B., Watt, P.B. & Cohen, P. (1990) *Nature (London)* **348**, 302-308.
49. Ullrich, A. & Schlessinger, J. (1990) *Cell.* **61**, 203-212
50. Pallotta, B.S. (1991) FASEB J. **5**, 2035-2043.
51. Colquhoun, D. & Sakmann, B. (1985) *J. Physiol. (London)* **369**, 501-557.
52. Montal, M., Labarca, P., Fredkin, D.R., Suarez-Isla, B.A. & Lindstrom, J. (1984) *Biophys. J.* **45**, 163-174.
53. Siara, J., Ruppersberg, J.P. & Rudel, R. (1990) *Pflügers Arch.* **415**, 701-706.
54. Downing, J.E.G. & Role, L.W. (1987) *Proc. Natl. Acad. Sci. USA* **84**, 7739-7743.
55. Green, W.N., Ross, A.F. & Claudio, T. (1990) *Neuron* **7**, 659-666.
56. Ross, A.F., Green, W.N., Hartman, D.S. & Claudio, T. (1991) *J. Cell Biol.* **113**, 623-636.
57. Green, W.N., Ross, A.F. & Claudio, T. (1991) *Proc. Natl. Acad. Sci. USA* **88**, 854-858.
58. Wittekind, M., Reizer, J., Deutscher, J., Saier, M.H. & Klevit, R.E. (1989). *Biochemistry* **20**, 9908-9912.
59. Murphy, B.J. & Catterall, W.A. (1992) *J. Biol. Chem.* **267**, 129-134.
60. I i, M., West, J.W., Scheuer, T. & Catterall, W.A. (1992) *Neuron* **8**, 1157-1159.
61. West, J.W., Numann, R., Murphy, B.J., Scheuer, T. & Catterall, W.A. 91992) *Biophys. J.* **62**, 31-33.
62. West, J.W., Numann, R., Murphy, B.J., Scheuer, T. & Catterall, W.A. (1991) *Science* **254**, 866-868.
63. Schreibmayer, W., Dascal, N., Lotan, I., Wallner, M. & Weigl, L. (1992) *FEBS Lett.* **291**, 341-344.
64. Dascal, N. & Lotan, I. (1991) *Neuron* **6**, 165-175.
65. Ahmed, C.M.I., Ware, D.H., Lee, S.C., Patten, C.D., Ferrer-Montiel, A.V., Schinder, A., McPherson, J.P., Wagner-McPherson, K., Wasmuth, J.J., Evans, G.A. & Montal, M. (1992) *Proc. Natl. Acad. Sci USA* **89**, 8220-8224.
66. Feng, D.F. & Doolittle, R.F. (1990) *Methods Enzymol.* **183**, 375-387.
67. Greenblatt, R.E., Blatt, Y. & Montal, M. (1985) *FEBS Lett.* **193**, 125-134.
68. Guy, H.R. & Conti, F. (1990) *Trends Neurosci.* **13**, 201-206.
69. Gavel, Y. & von Heijne, G. (1990) *Protein Eng.* **3**, 433-442.
70. Glass, D.B., El-Maghrabi, M.R. & Pilkis, S.J. (1986) *J. Biol. Chem.* **261**, 2987-2993.
71. Kishimoto, A., Nishiyama, K., Nakanishi, H., Uratsuji, Y., Nomura, H., Takeyama, Y. & Nishizuka, Y. (1985) *J. Biol. Chem.* **260**, 12492-12499.
72. Hodgkin, A.L. & Huxley, A.F. (1952) *J. Physiol. (London)* **116**, 497-506.
73. Hille, B. (1992). *In: Ionic Channels of Excitable Membranes*. 2nd ed. (Sinauer Associates, Sunderland, MA).

5. Appendix A

Table 1. Single-channel properties of purified AChR

		Protein kinase A-activated		
	Spontaneous	0.3 mol of phosphate per mol of AChR	1.0 mol of phosphate per mol of AChR	ACh-activated†
p_o, %	0.08 ± 0.07	0.5 ± 0.4*	2.9 ± 3.0*	14 ± 6
γ, pS	44 ± 6	47 ± 8****	45 ± 7****	45 ± 2
τ_{OS}, ms‡	0.10 ± 0.05	0.2 ± 0.1**	0.6 ± 0.4**	0.5 ± 0.1
τ_{OL}, ms	0.9 ± 0.4	2.5 ± 1.7**	3.4 ± 2.8**	3.8 ± 0.3
A_{OL}/A_{OS}	0.08 ± 0.07	0.3 ± 0.2***	0.4 ± 0.5***	0.25 ± 0.09
τ_{CS}, ms‡	4 ± 2	3 ± 1****	2 ± 2****	1.1 ± 0.1§
τ_{CL}, ms	1373 ± 1041	1041 ± 1016****	480 ± 600***	5.4 ± 0.6
A_{CL}/A_{CS}	8 ± 4	3 ± 1****	3 ± 5***	1.2 ± 0.5

Segments of records with durations of 102 s were analyzed. Values are given as mean ± SD. Statistical comparison of the protein kinase A-activated AChR with respect to the spontaneous channel activity using the nonparametric Mann-Whitney rank sum test (46) showed the following significance values: $P < 0.0002$; the total number of events analyzed, n, was ≥ 3500; the number of experiments, N, was N = 11, 15 and = 6 for spontaneous and kinase A-activated with stoichiometries of 0.3 and 1.0 mol of phosphate per mol of AChR, respectively. **, $P < 0.007$; n ≥ 2500; N = 6, 7, and 6. ***, $P < 0.02$; n ≥ 2500; N = 6, 7, and 6. ****, $P > 0.05$; n ≥ 2500; N = 6, 7, and 6.

†ACh was 1 μM. Segments of records with durations of 30 s were analyzed. n = 4790; N = 11.

‡Open and closed dwell times were calculated as described.

§Closed times were fitted with three exponential components (7). The time constant and amplitude of the third component were $\tau_{C3} = 33 \pm 5$ ms and $A_{C3} = 0.11 \pm 0.04$.

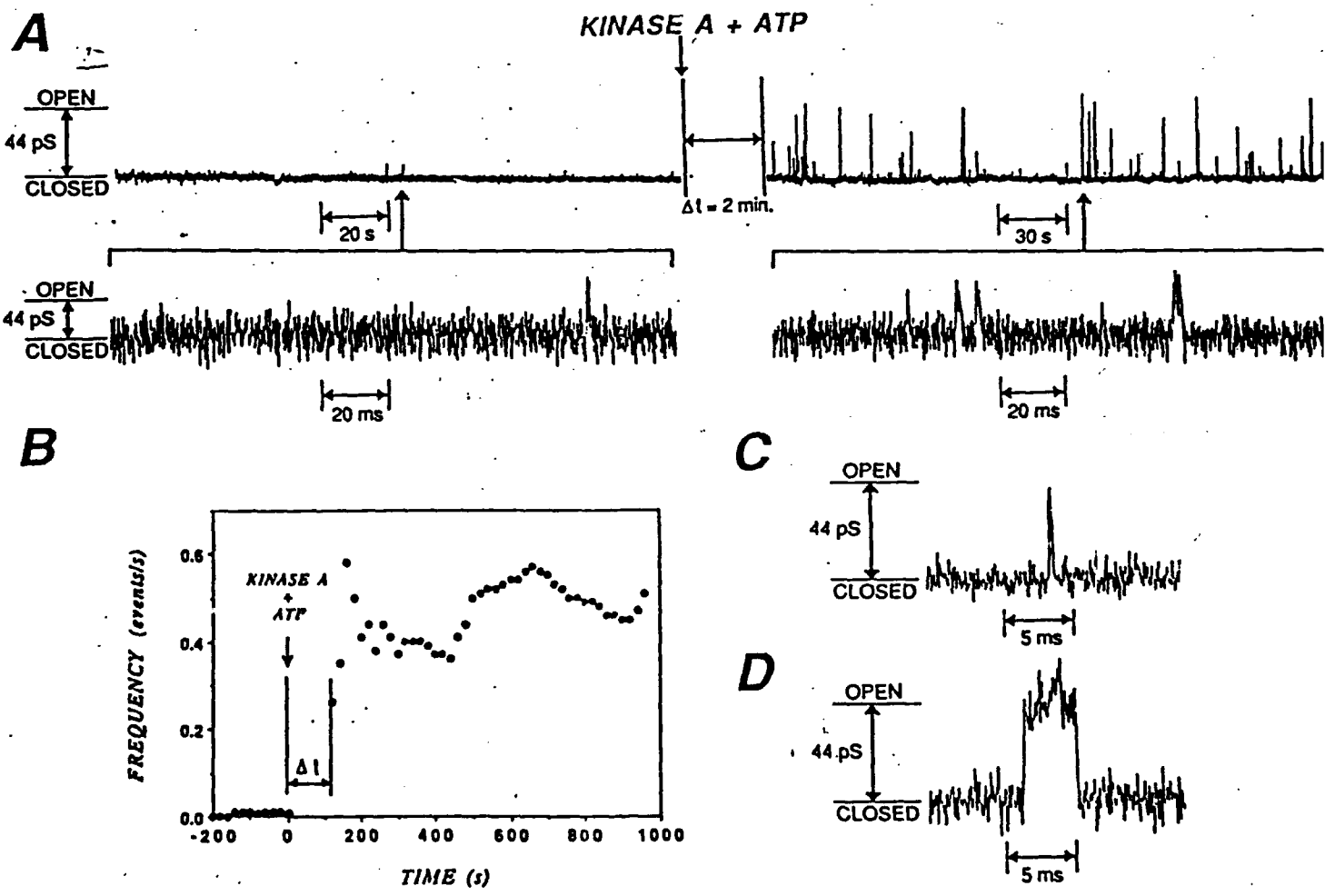

Figure 1. Activation by catalytic subunit of protein kinase A of AChR channels reconstituted in lipid bilayers A: Single channel current at 50 mV in absence of ACh before and after addition to the bath of purified recombinant catalytic subunit of kinase A from murine heart (17) (5 μg/ml) and ATP (200 μM). The display is interrupted (Δt = 2 min.) to allow for equilibration of reactants. The sectors indicated by arrows are shown at higher resolution. B: Time course of the increase in opening frequency following addition of protein kinase A and ATP. Number of channel openings was counted at 20 s intervals and the accrued value divided by the elapsed recording time. Other conditions as in A. C and D. Single AChR channel currents displayed at higher resolution for the two groups, before (C) and after (D) protein kinase A addition. Records were filtered either at 50 Hz (A, Upper) or 2 kHz (A, Lower) or 1.25 kHz (C and D) and digitized at a sampling rate of 100 Hz (A, Upper) and 10 kHz (A, Lower and C and D).

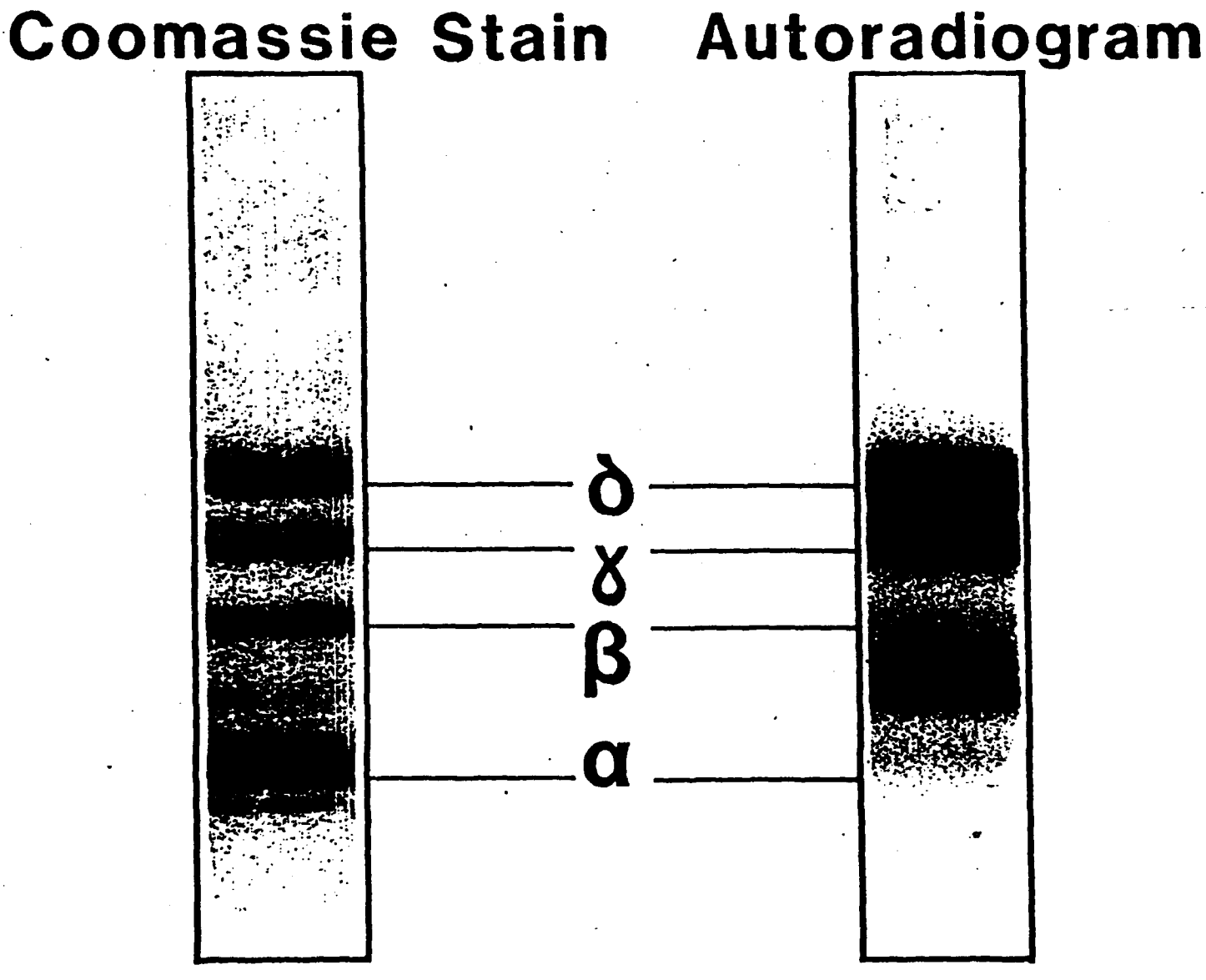

Figure 2. Phosphorylation of purified *Torpedo californica* AChR γ and δ subunits by protein kinase A. Coomassie-stained gel (Left) shows the four protein subunits of the receptor; autoradiogram (Right) shows the distribution of ^{32}P. The extent of phosphorylation shown was 0.11 and 0.10 mol of ^{32}P per mol of γ and δ subunit, respectively.

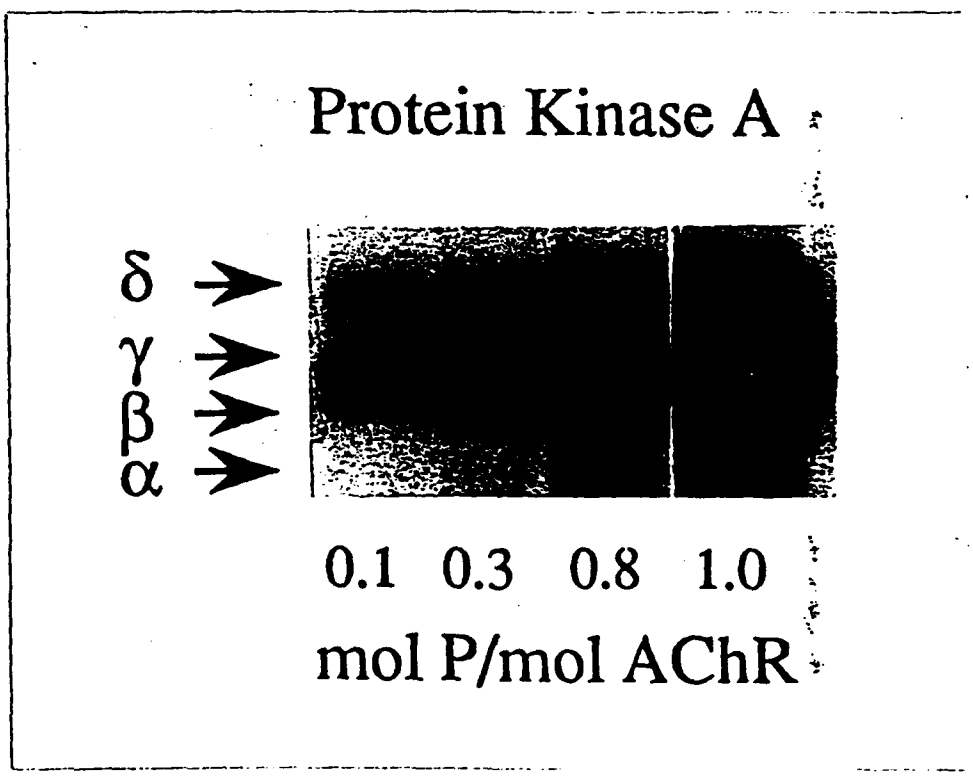

Figure 3. Phosphorylation stoichiometery of *Torpedo californica* AChR γ and δ subunits. Autoradiograms of gels processed as described in Fig. 2 show the extent of ^{32}P-labeling of AChR subunits resulting from exposure to kinase A and ATP for progressively longer periods. The resultant stoichiometries of mol phosphate/mol AChR are indicated. The incubation conditions used were: 1 min with 6.5 mU/ml of PKA for 0.1 mol phosphate/AChR; 5 min with 6.5 mU/ml of PKA for 0.3 mol phosphate/AChR; 15 min with 6.5 mU/ml of PKA for 0.8 mol phosphate/AChR, and 1 min with 65 mU/ml of PKA for 1.0 mol phosphate/AChR.

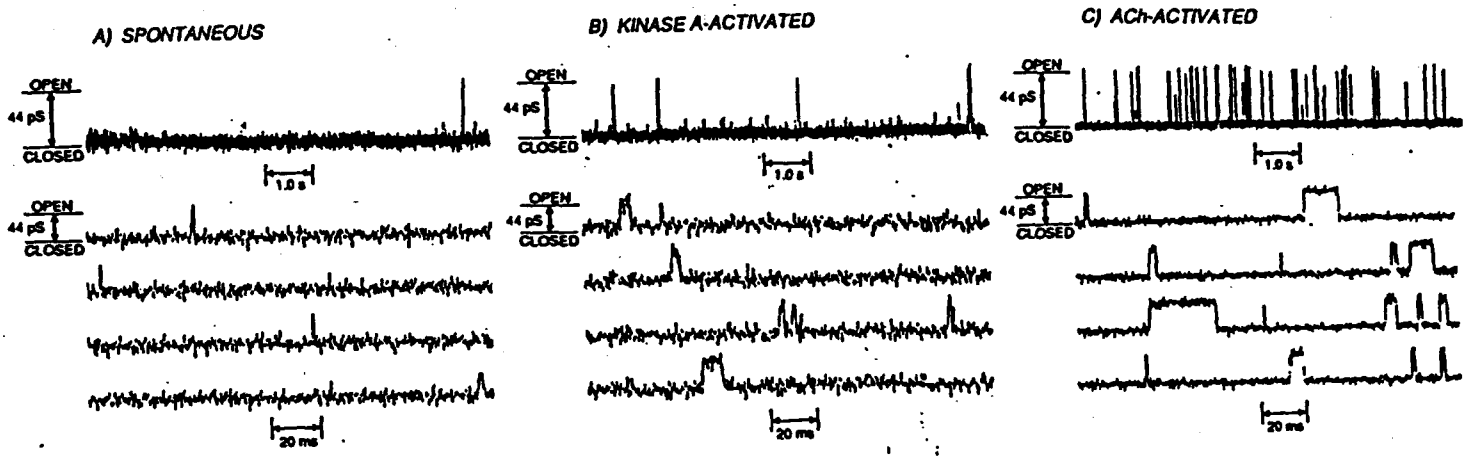

Figure 4. Single-channel currents from purified *Torpedo californica* AChR reconstituted in lipid bilayers. A: Spontaneous activity recorded at 50 mV in absence of ACh. B: AChR phosphorylated *in vitro* by protein kinase A to a stoichiometry of 0.3 mol of phosphate per mol of AChR; currents were recorded at 50 mV in absence of ACh. C: Unphosphorylated AChR; currents activated by 1 μM ACh and recorded at 100 mV. (Lower) Four representative sweeps at higher resolution. Data were filtered at 1 kHz.

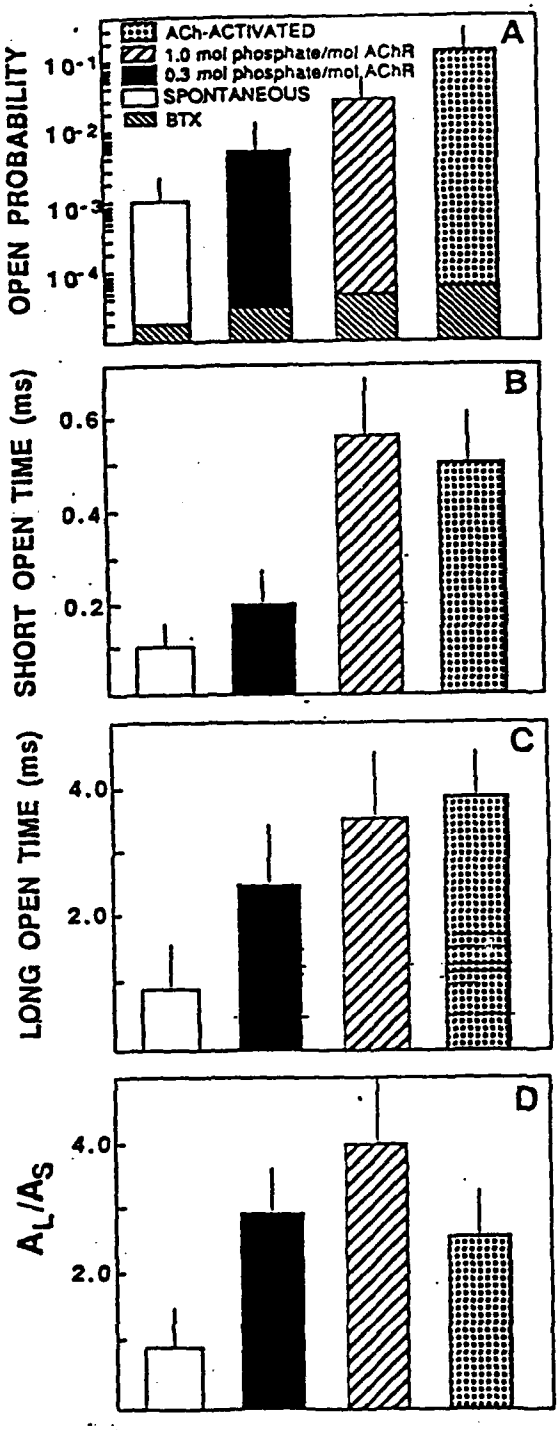

Figure 5. Probability density analysis of dwell times in the open state recorded at 50 mV for spontaneous, and protein kinase A-activated, and 100 mV for ACh-activated AChR channels. A: Probability of channel opening. B and C: Time constants for the short and long components of the probability density distribution, respectively. D: Ratio of the areas under the fitted probability densities. For ACh-activated channels, ACh was 1μM in absence or presence of 200nMBTX inside the pipet. For spontaneous, and protein kinase A-activated channels, 200nMBTX was present in the two aqueous compartments separated by the membrane, as indicated. Values are given as mean ± SEM.

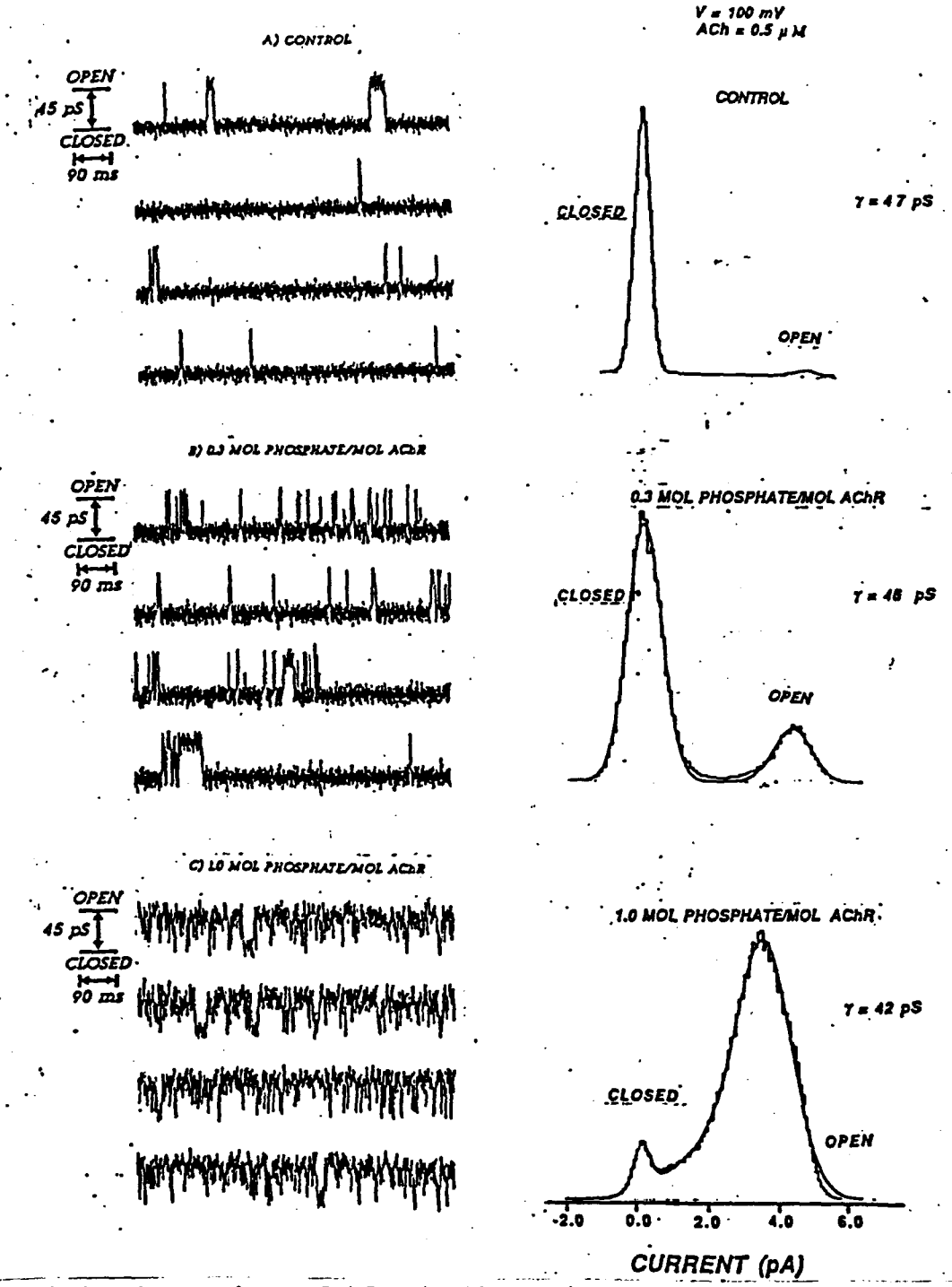

Figure 6A. Single-channel currents from purified *Torpedo californica* AChR reconstituted in lipid bilayers in the unphosphorylated (*A*) and phosphorylated form (*B,C*). AChR channels were activated by 0.5 μM ACh and recorded at V= 100 mV. The aqueous phase contained 0.5 M KCl and 1 mM $CaCl_2$. Four segments of 0.8 second duration are illustrated for each condition. The control shown in (*A*) was obtained under identical conditions to the phosphorylated samples (*B,C*) with the exception that PKA was omitted. The stoichiometery of phosphorylation was 0.34 and 1.0 mol phosphate/mol AChR for records B, and C, respectively. Data were filtered at 2 kHz and digitized at 0.1ms/point. Other conditions as for Fig. 1.

Figure 6B. Single-channel current histograms corresponding to the experimental samples presented in Fig. A for the control and phosphorylated AChR. Histograms of 15 sec segments of recordings in which only one channel was open at any given time were analyzed. Fitted Gaussian distributions (smooth curves) are superimposed over the experimental histograms (noisy curves) and correspond to the channel closed state (peak at zero current) and the open state (peaks at 4.7 pA, 4.6 pA, and 42pA, respectively for A, B, and C). Calculated γs are 47 pS, 46 pS and 42 pS, respectively. The area under the fitted curves correspond to the probability of occurrence of that state. The open probability, P_O, for the unphosphorylated sample (A) was 4%. For the phosphorylated samples, P_O was 16% and 95%, for B, and C, respectively. Other conditions were as for Fig. 5.

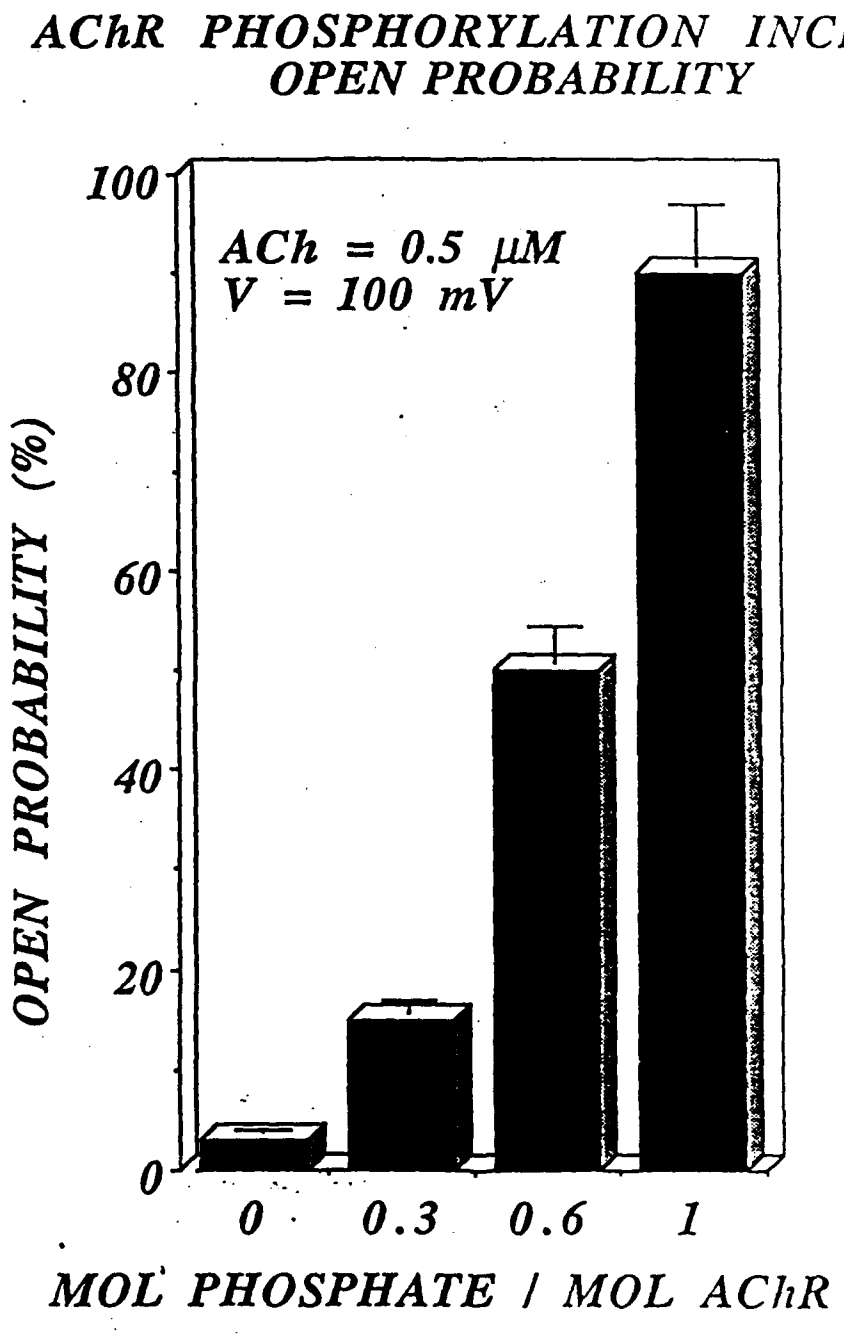

Figure 7. Probability of single AChR channel opening as function of phosphorylation stoichiometry. Data pooled from eight different experiments recorded at V=mV and activated by 0.5 μM ACh. Open probability was calculated as described in Fig. 6. Other conditions as for Fig. 5.

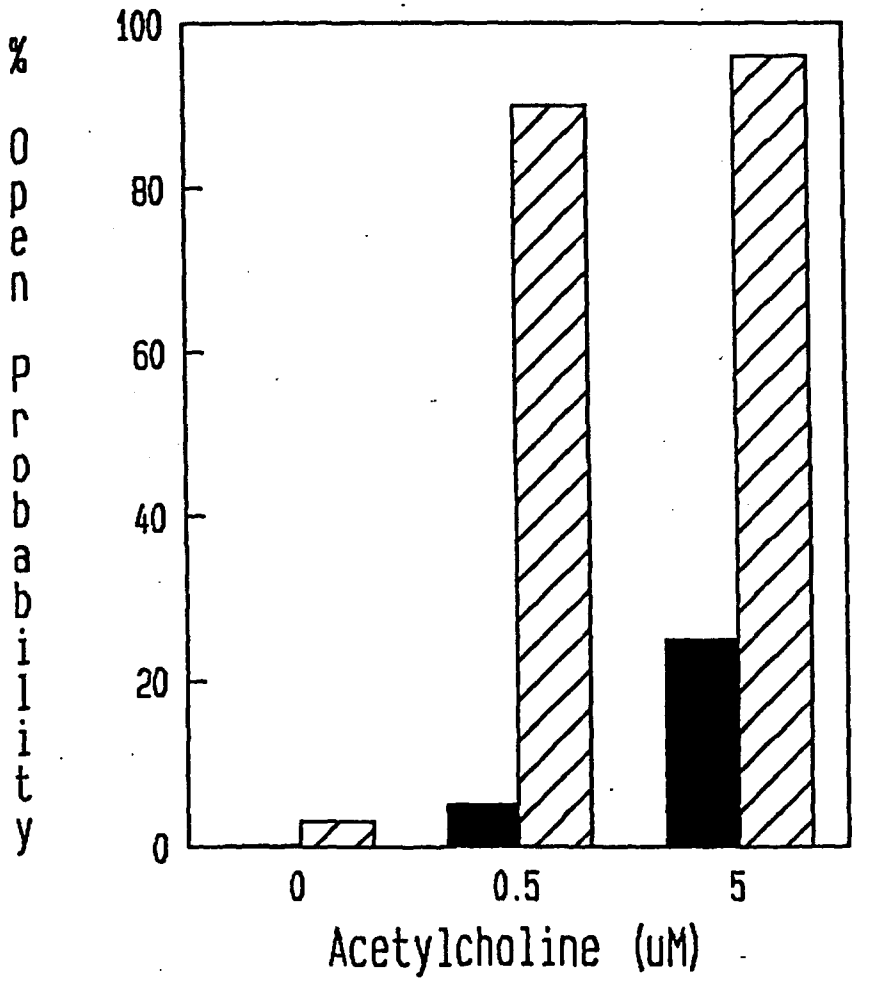

Figure 8. Probability of single AChR channel opening as a function of ACh concentration at a fixed stoichiometry of 1.0 mol phosphate/mol AChR. Data compiled from five different experiments recorded at V = 100mV. Open probability was calculated as described in Fig. 5. Filled bars represent unmodified AChRs and stripped bars, phosphorylated AChRs.

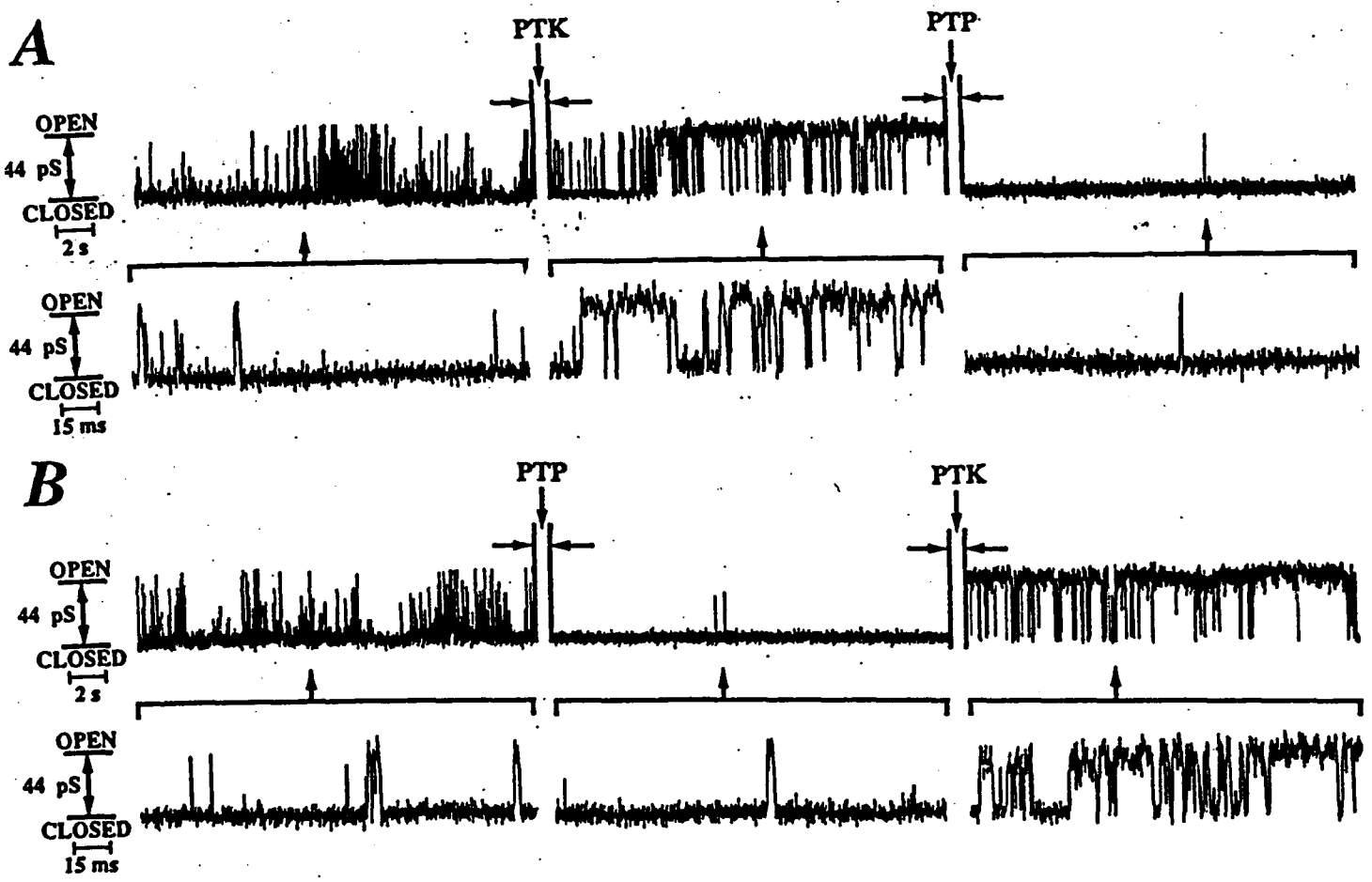

Figure 9. Tyrosine-specific kinase and phosphatase reversibly modify *Torpedo californica* AChR channel activity. AChR channels were activated by 1 μM ACh and recorded at 100mV. A: Current recordings from unmodified (control) AChR are illustrated (left panel). The middle display shows the increase in AChR channel activity after the addition of PTK (20 U/ml); the record in the right shows that simultaneous addition of 12 mM EGTA/KOH pH 7.4 (to arrest the kinase activity) and PTP (5 U/ml) abate AChR channel activity. B: Initial sector illustrates activity of unmodified AChR. The middle trace displays the decrease of AChR activity consequent to PTP addition (5 U/ml); the record on the right shows that simultaneous addition of 100 μM $(NH_3)_6Mo_7O_{24}$ (to cessate PTP activity) and PTK (20 U/m) augment AChR channel activity. Gaps represent interruptions in the records (2-4 min), to allow equilibration of reagents in the bilayer chamber. Records were filtered at 50 Hz or 2 kHz, and digitized at sampling rate of 50 Hz or 10 kHz for the compressed and expanded records, respectively. The effects of both enzymes on AChR channel activity were strictly dependent on the presence of 0.1% β-mercaptoethanol in the external bath solution (data not shown).

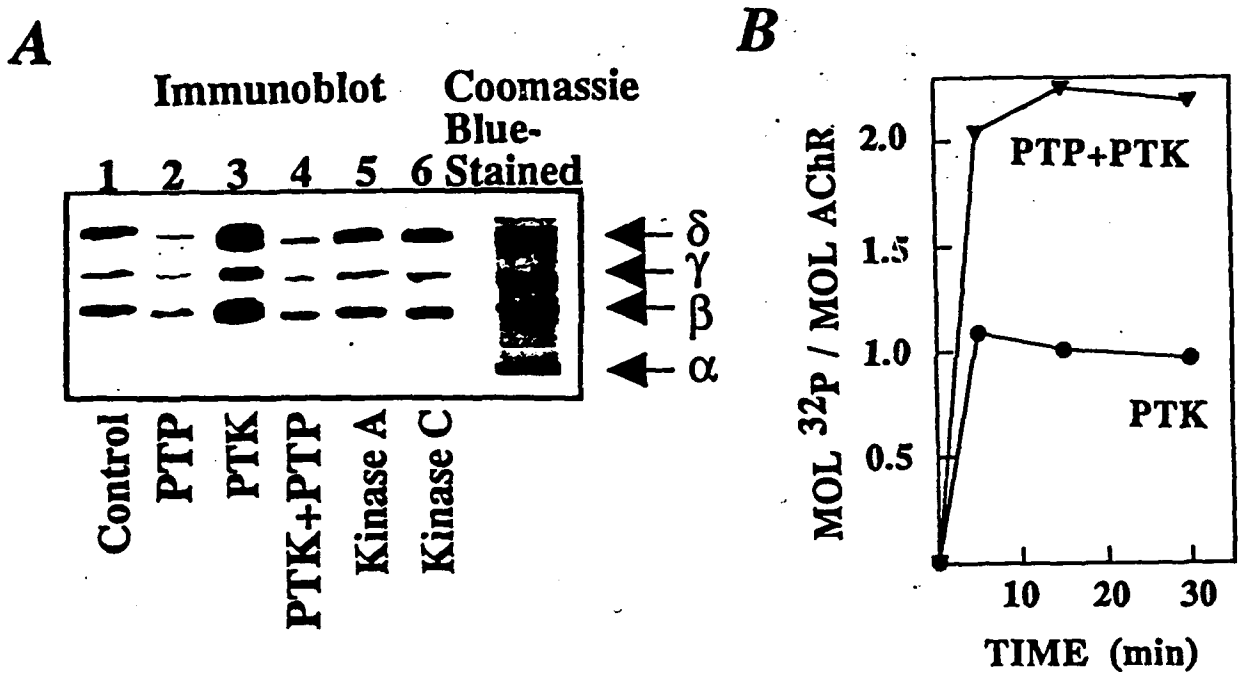

Figure 10. Protein tyrosine phosphorylation and dephosphorylation of *Torpedo californica* AChR subunits. A: Immunoblot detection of AChR phosphotyrosines using a monoclonal antiphosphotyrosine antibody. Lane 1: Endogenous AChR phosphotyrosines in β,γ, δ subunits. Lanes 2-6 show extent of AChR phosphotyrosine after treatment with PTP (Lane 2); PTK (Lane 3); PTK followed by PTP (Lane 4); Recombinant catalytic subunit of protein kinase A (Lane 5); Protein kinase C (Lane 6). Lane 7: Coomassie blue-stained gel showing the 4 subunits of the AChR, with apparent molecular weights of: α, 40,000; β, 50,000; γ, 58,000; and δ, 64,000. B: Time course of ^{32}P incorporation to unmodified (●) and PTP- dephosphorylated (▼) AChRs after PTK treatment.. Values represent extent of ^{32}P incorporation into β, γ and δ subunits; means of two independent determinations with error ≤ 10%.

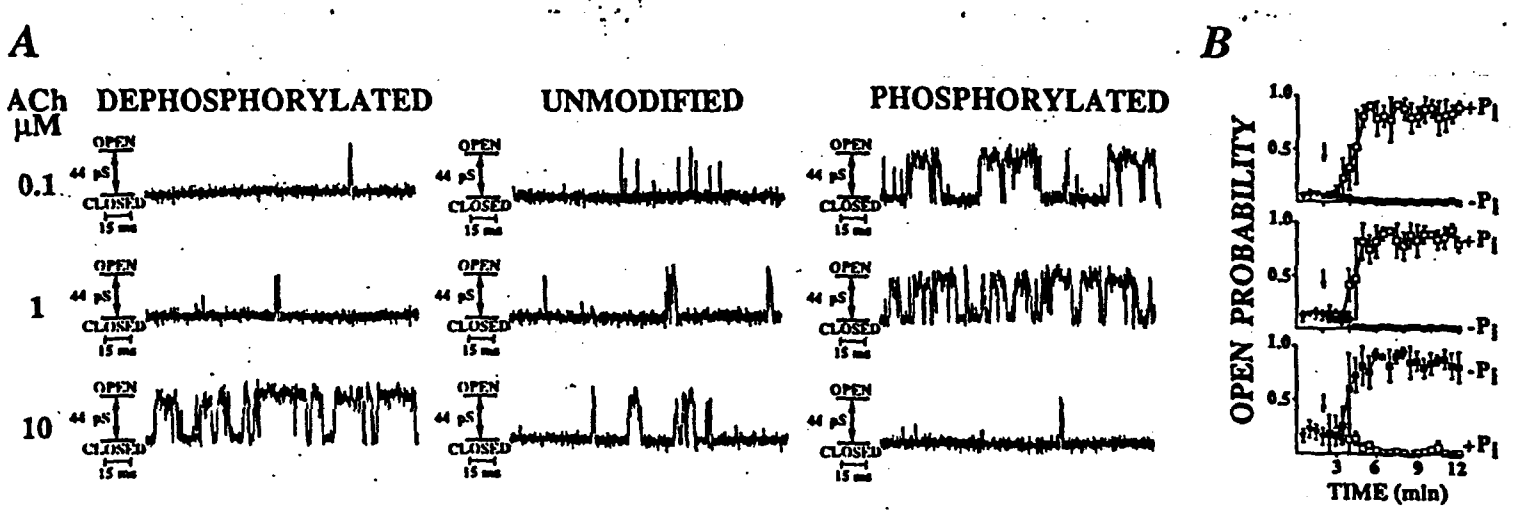

Figure 11. Protein tyrosine phosphorylation/dephosphorylation and agonist concentration concertedly modulate *Torpedo californica* AChR channel activity. Panel A illustrates channel activity of dephosphorylated, unmodified, and phosphorylated AChRs in presence of 0.1, 1, and 10 μM ACh, respectively. AChR channel activity was recorded at 100 mV, filtered at 2 kHz and digitized at 10 kHz. Panel B shows the time course of channel open probability elicited by the PTK and PTP enzymatic treatments, indicated as +Pi and -Pi, at 0.1, 1 and 10 μM ACh. Arrows indicate the onset of enzymatic treatment. Plotted values are mean ± SEM, n ≥ 3; n, denotes number of experiments; each value calculated for recordings with N ≥ 520, where N denotes number of events. Other conditions were as described in Fig. 9.

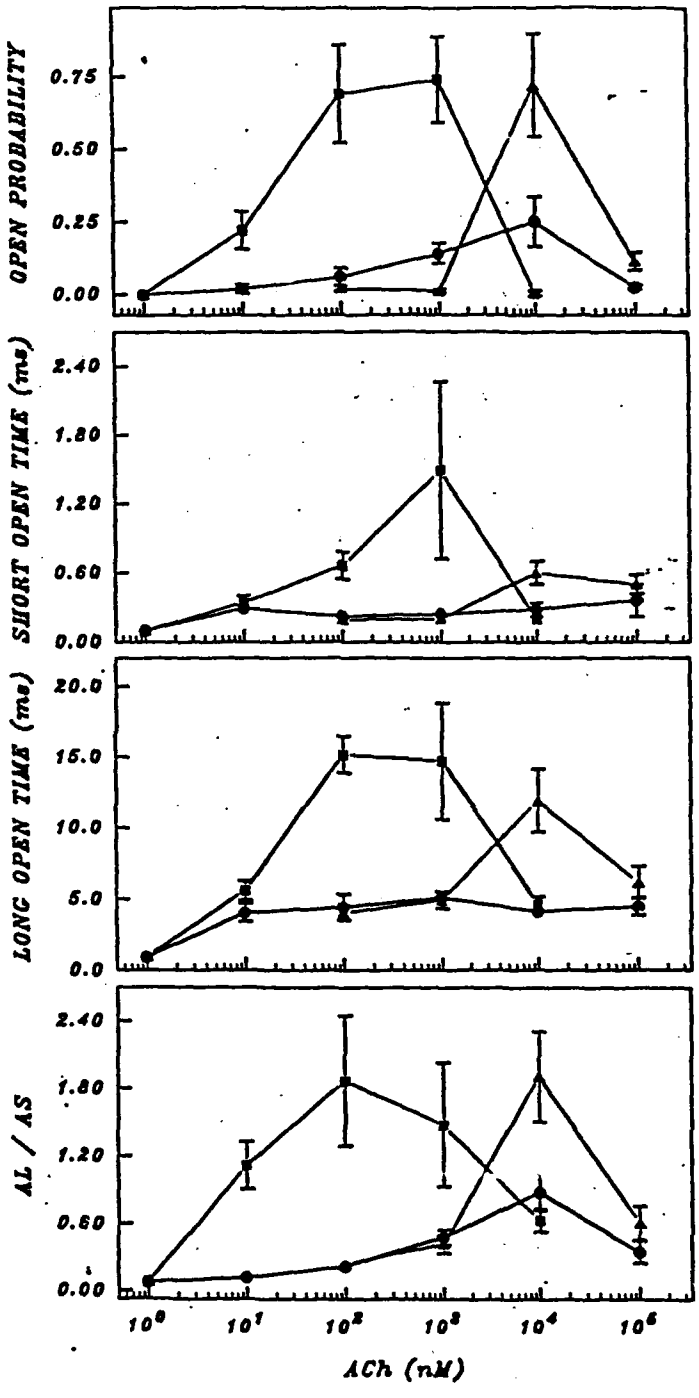

Figure 12. ACh concentration-dependence of channel open probability and kinetic parameters of dwell times in the open state for unmodified (●), tyrosine phosphorylated (■) and tyrosine dephosphorylated (▼) *Torpedo californica* AChR. (A) Channel open probability. (B and C) Time constants for the short and long components of the probability density distribution, respectively. (D) Ratio of the areas under the fitted probability densities. Values are mean ± SEM, n ≥ 3; calculated values for N≥1050 per tabulated point. Values displayed at 10^{-9} M ACh represent the spontaneous AChR activity (18). Records were filtered at 5 kHz and digitized at 50 μs/point). Other conditions were as described in Fig. 9

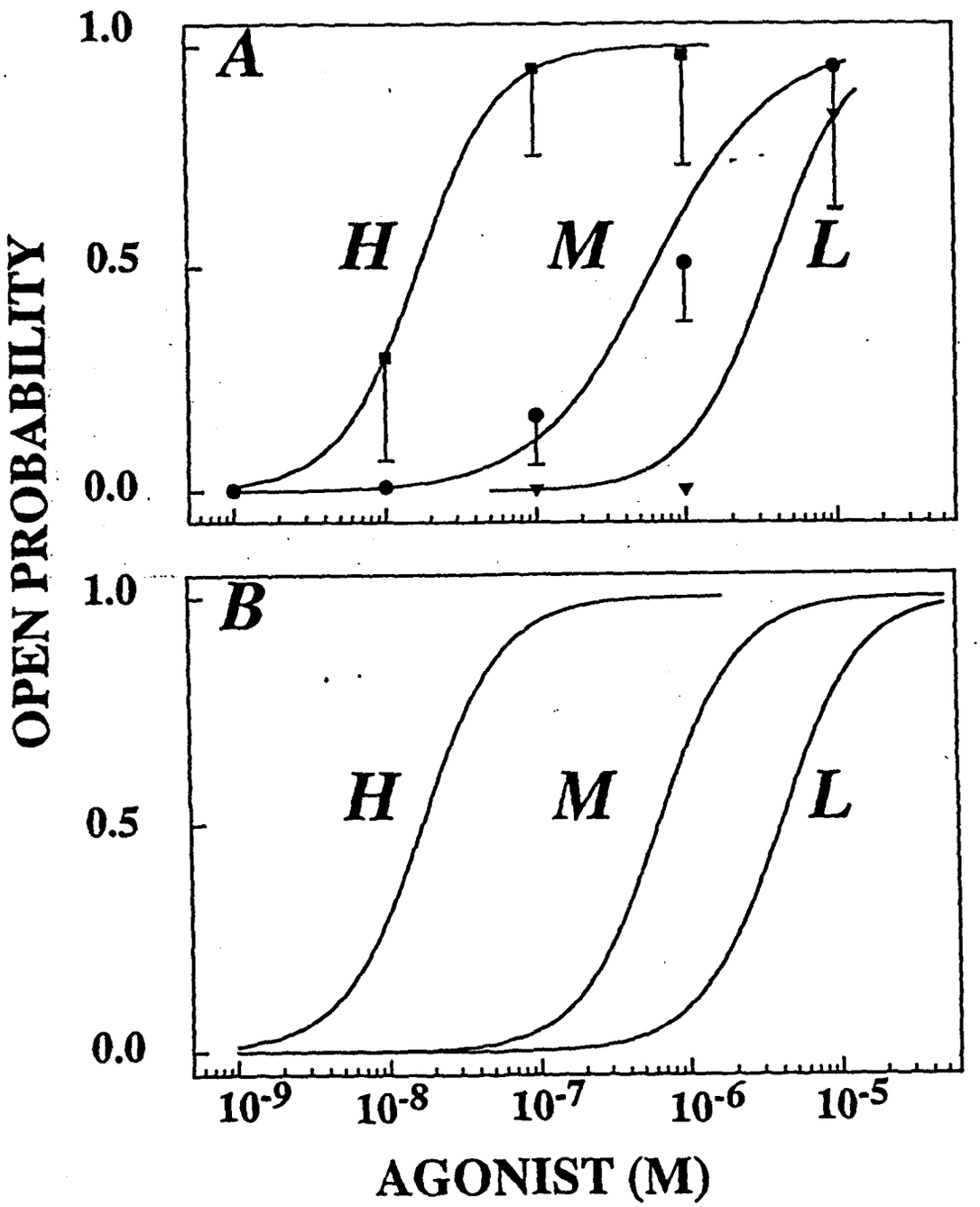

Figure 13. Tyrosine-phosphorylation regulates the sensitivity of AChR for its agonist. A: Dose-response curves for ACh of unmodified (●, (M)edium degree of phosphorylation), phosphorylated (■, (H)igh degree of phosphorylation) and dephosphorylated (▼, (L)ow degree of phosphorylation) AChRs. Y-axis denotes the normalized open probability calculated from the values displayed in Fig. 4, panel A. Solid lines depict theoretical fits to a Michaelis-Menten binding isotherm given by $P/P_{max} = K\,[\text{agonist}]^n/(1+K\,[\text{agonist}]^n)$, where P is the open probability at a given agonist concentration, K is the affinity constant for the agonist concentration at which probability is half-maximal (P_{max}), and n is the number of ligand binding sites. To normalize, *Pmax* was obtained from the best-fit to the above equation using the values of Fig. 4. B: Dose-response curves for three hypothetical agonists of the AChR with (H)igh, (M)edium, and (L)ow binding affinities

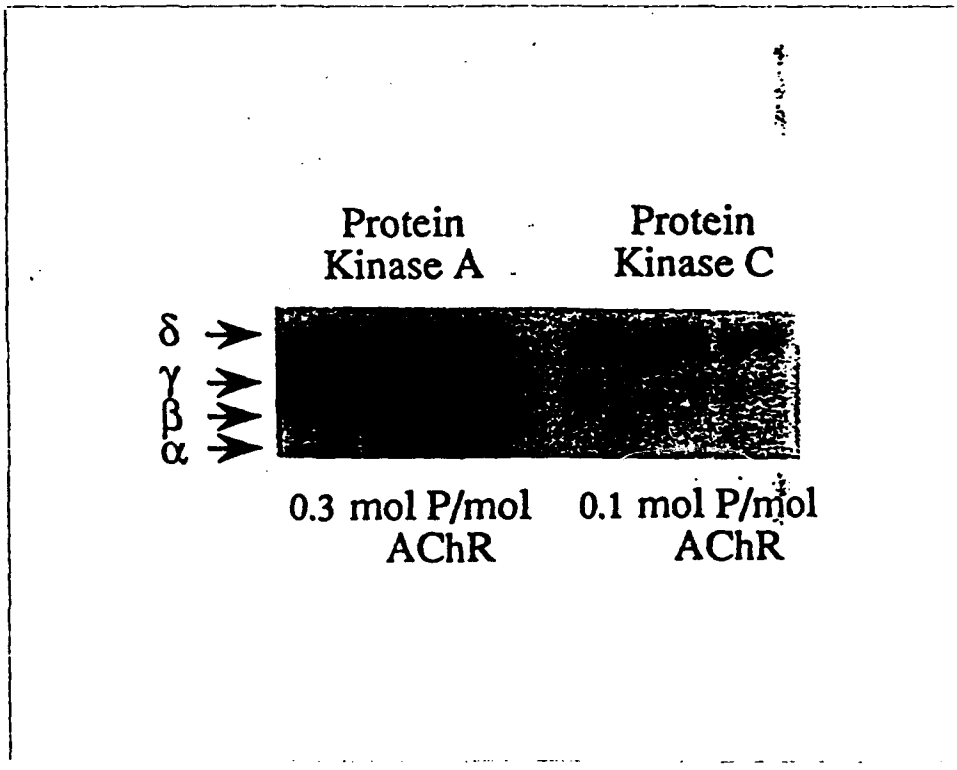

Figure 14. Phosphorylation of purified *Torpedo californica* AChR subunits by protein kinase A and protein kinase C, as indicated. Autoradiograms of SDS/PAGE gels showing the distribution of ^{32}P. Each experiment was done in triplicate. AChR phosphorylation by protein kinase A is preferentially on γ and δ subunit whereas primarily δ is labeled by protein kinase C. Phosphorylation by protein kinase C was as indicated in Fig. 3 for the stoichiometry of 0.3 mol phosphate/AChR (namely, incubation of 5 min with 6.5 mU/ml of PKA to yield a stoichiometry of 0.3 mol phosphate/mol AChR). for PKC phosphorylation the incubation medium contained, in addition, 20 μM $MgCl_2$, 2mM $CaCl_2$ and 1.5 U/ml of protein kinase C. The reaction proceeded for 20 min. Other conditions as for Fig. 2 and 3.

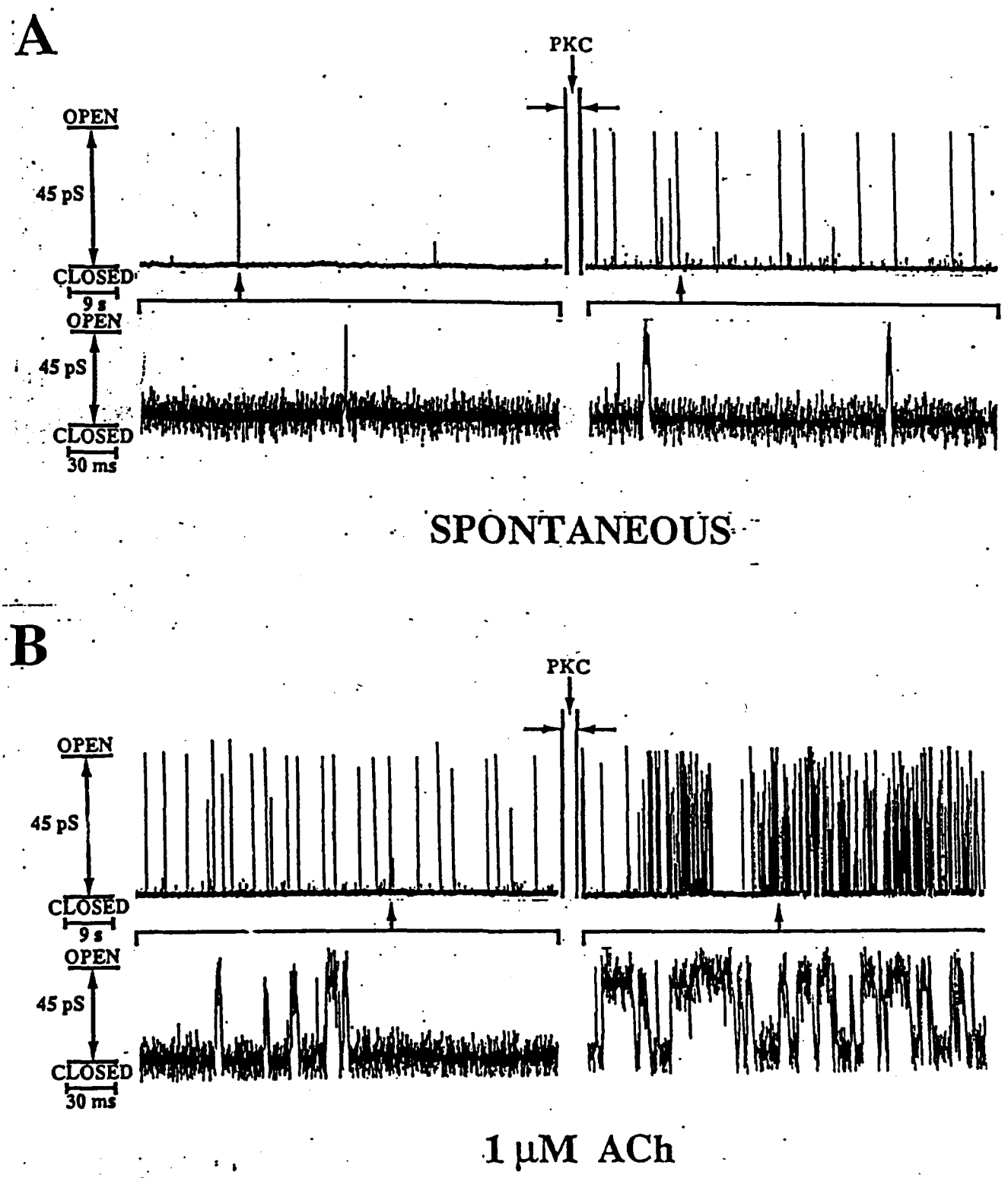

Figure 15. Protein kinase C activates AChR channels reconstituted in lipid bilayers. A: Single-channel currents at 100mV in the absence of ACh before and after addition to the bath of protein kinase C (0.3 U/ml). The display is interrupted (Δt = 5 min) to allow for equilibration of reactants. The sectors indicated by arrows are shown at higher resolution. B: Recordings obtained in the presence of 1 μM ACh inside the pipet before and after addition of protein kinase. Other conditions are the same as in A. Records were filtered at 50 Hz (Upper) and 2 kHz (Lower) and digitized at a sampling rate of 100 Hz (Upper) and 10 kHz (Lower). The aqueous buffered composition as 0.5 M KCl, 5 mM $CaCl_2$, 12 mM $MgCl_2$, 10 mM Hepes, pH 7.4, 250 μM ATP and 0.1% β-mercaptoethanol.

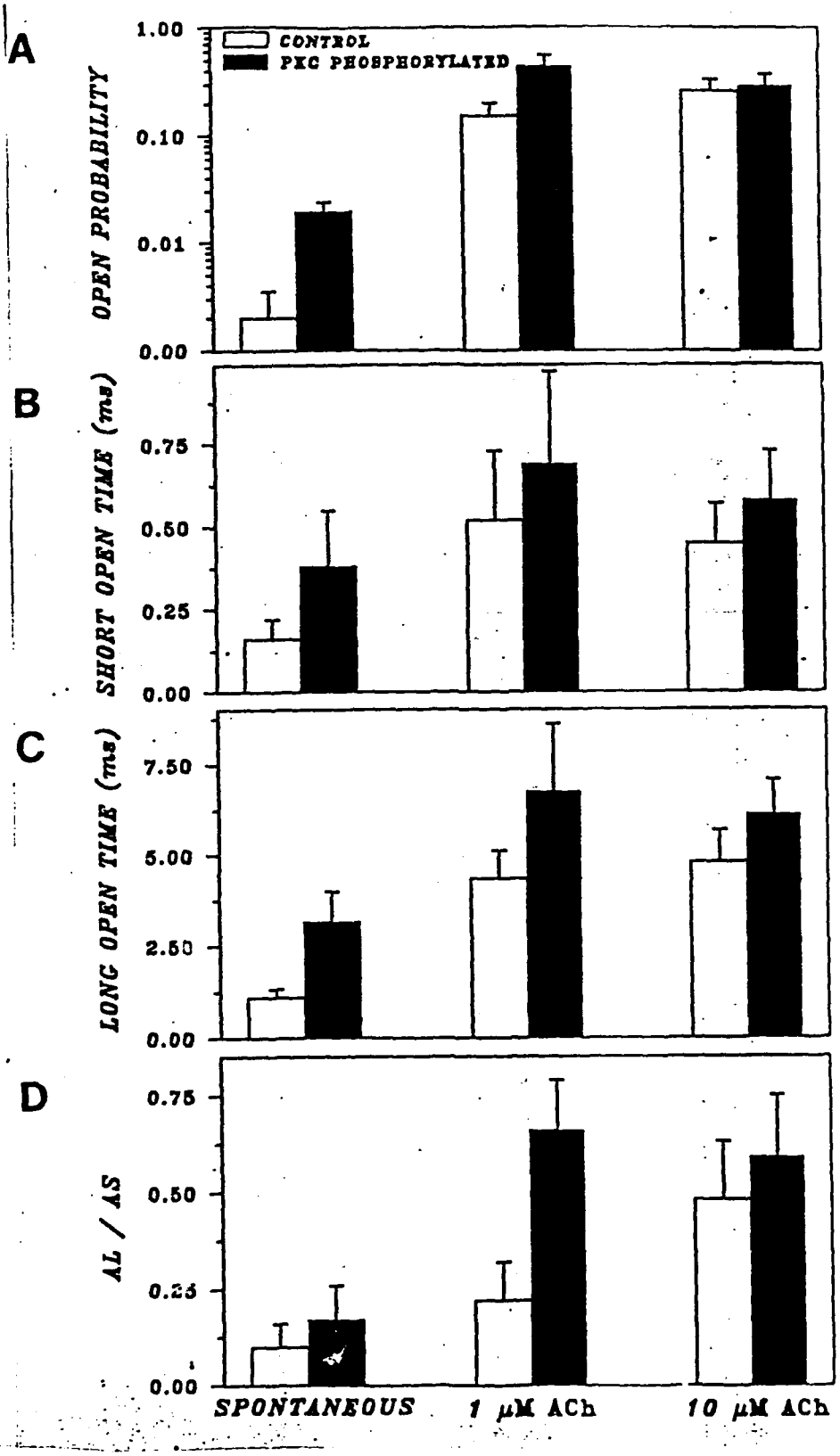

Figure 16. Probability density analysis of dwell times in the open state recorded at 100 mV for spontaneous and ACh-activated AChR channels before and after phosphorylation by protein kinase C (3 U/ml for 10 min at a stoichiometry of 0.1 mol phosphate/mol AChR). A: Probability of channel opening. B and C: Time constants for the short and long components of the probability density distribution. D: Ratio of the areas under the fitted probability densitiies. Values are given as means ± SEM (N ≥ 4 experiments; each determination with a minimum of 300 openings.

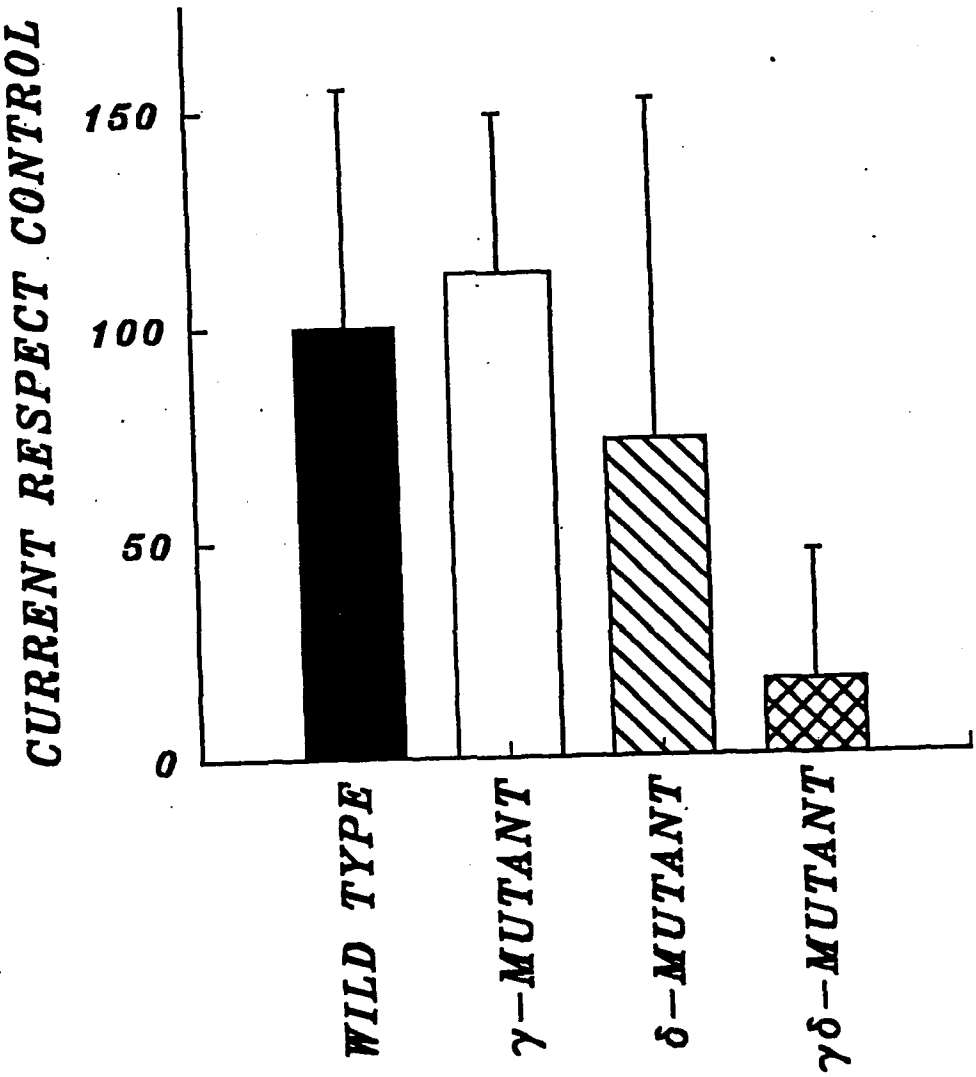

Figure 17. ACh-elicited currents in *Xenopus* oocytes expressing RNA transcripts of the *Torpedo* AChR wild-type and corresponding deletion mutants. For the γ subunit, the phosphorylation peptide (amino acid 353 to 371) was deleted corresponding to the removal of the nucleotide sequence encompassed between bp 1228-1285. for the δ subunit, the phosphorylation peptide (residue 360-379) was deleted corresponding to the removal of the DAN sequence encompassed between nucleotide 1598-1657. Oocytes were held at V = 60 mnV and continuously perfused with Ringer's solution. Pulses of ACh (50 μM) lasting 1 min were applied to ensure complete desensitization of the cholinergic response. Peak currents were used for the analysis. Values are given as means ± SEM (N = 10).

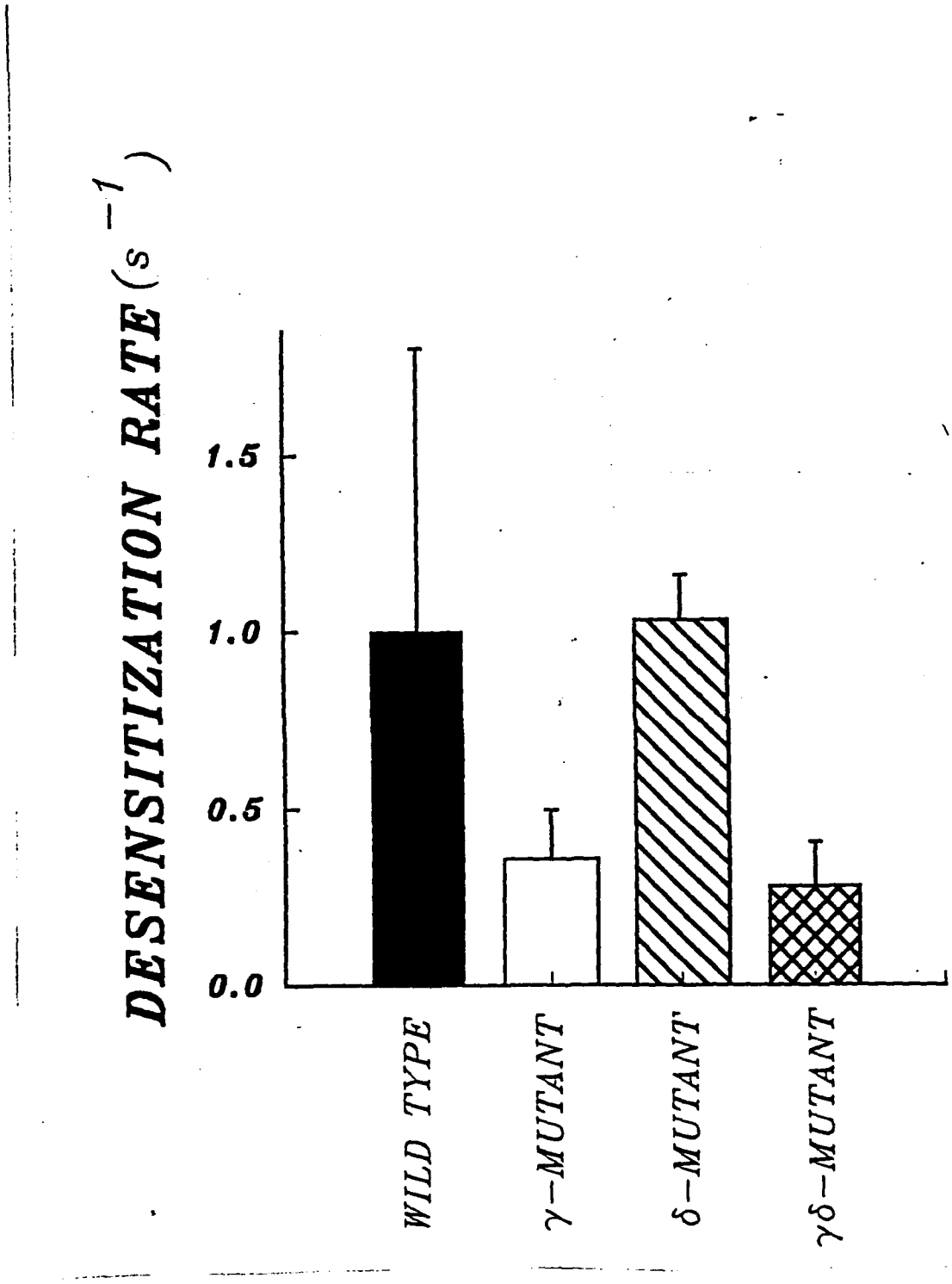

Figure 18. ACh-activated currents inactivation time for wild-type *Torpedo* AChR and the subunit specific deletion mutants expressed in *Xenopus* oocytes. Macroscopic currents were elicited by 50 μM ACh at a holding potential of -60 mV. The time to inactivate the peak current to 50% of its value is represented. Values are given as mean ± SEM (N = 10).

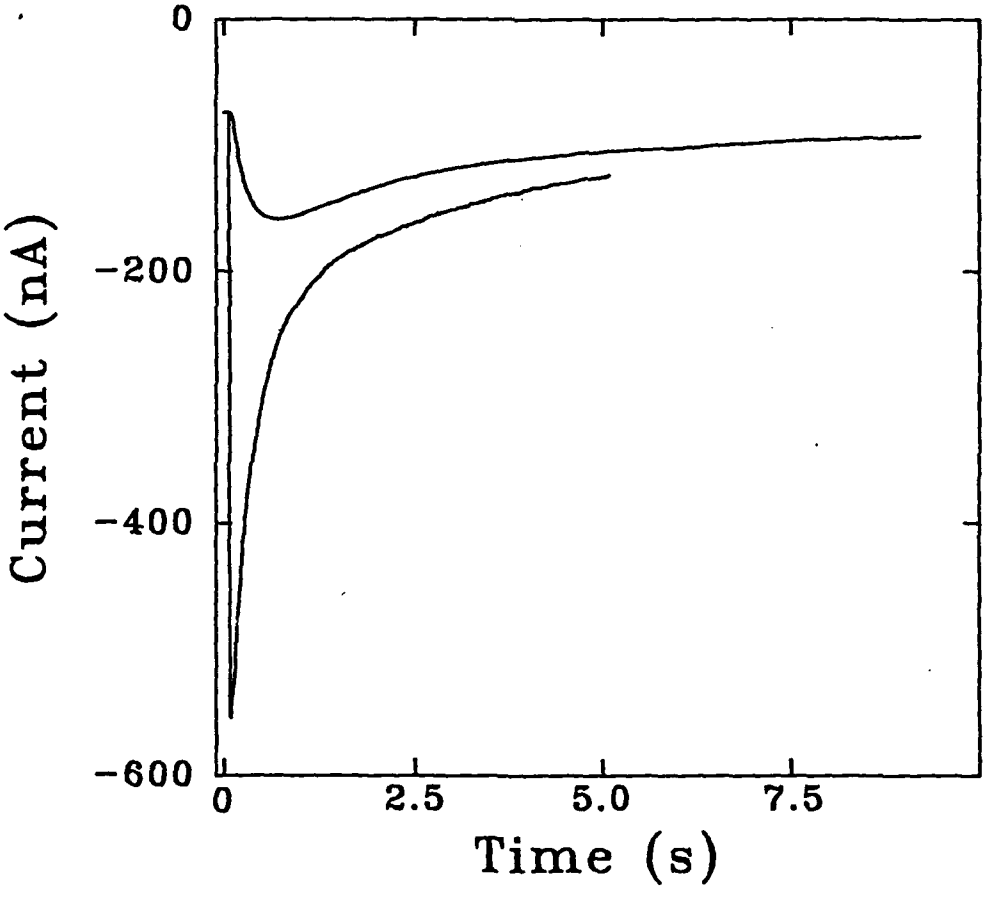

Figure 19. ACh-elicited currents in *Xenopus* oocytes expressing RNA transcripts of the AChRα7 cDNA from chicken brain. Oocytes were held at V = -80 mV and continuously perfused with Ringer's solution. Agonist was applied as indicated for 1 min in order to ensure the complete desensitization of the cholinergic response. ACh was 10 μM and 100 μM for the small and large amplitude current responses.

AChRα7	340	R R C **S** L S S M E M N T V S G Q Q C S N G N
AChRδ	358	R R C **S** S A G Y I A K A E E **Y** Y S V L **S** R S
AChRγ	350	R R R **S** S L G L M V K D E **Y** M A L W K A R

Figure 20. Alignment of the amino acid sequences containing the putative phosphorylation sites for neuronal α7 receptors from chicken brain, the AChRγ and δ subunits from chicken muscle. These phosphorylation sites are confined to a 22-amino acid stretch in the cytoplasmic loop connecting the predicted transmembrane segments M3 and M4. Amino acid residues modified by kinases are denoted in bold and underlined.

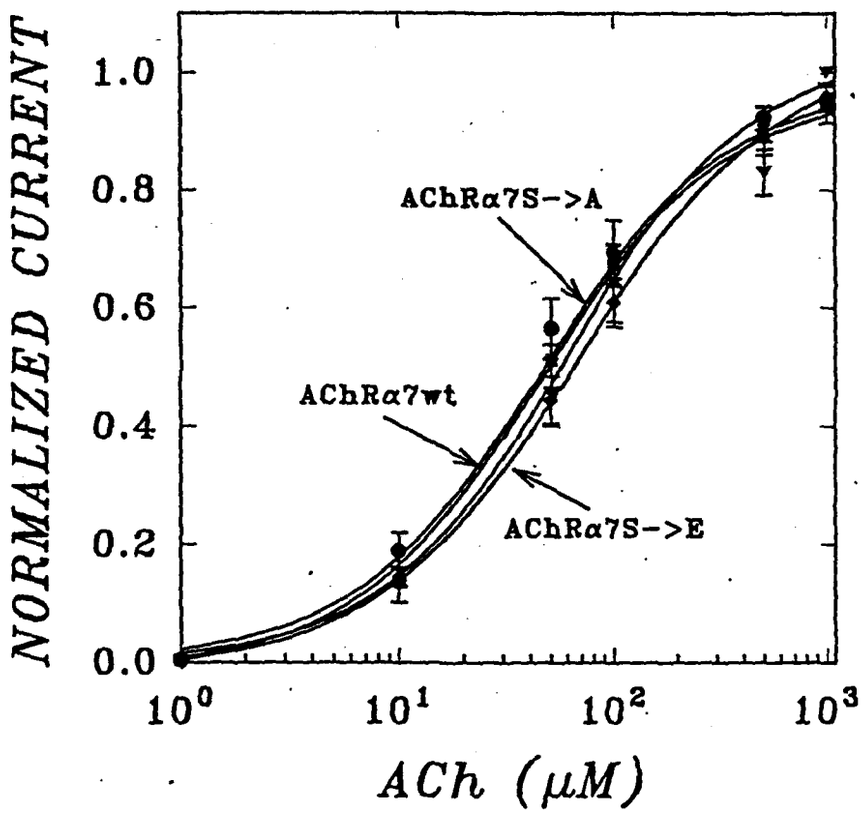

Figure 21. Dose-response curves for oocytes injected with cRNA transcripts of AChRα7 wild-type, AChRα7S →A mutant and AChRα7S → E mutant. Oocytes were held at V = -80 mV and ACh-currents were evoked as described in Fig. 20. Peak currents were used for this analysis. Each point represents mean±SD (N=11). Solid lines depict theoretical fits to a Michaelis-Menten Binding Isotherm (38).

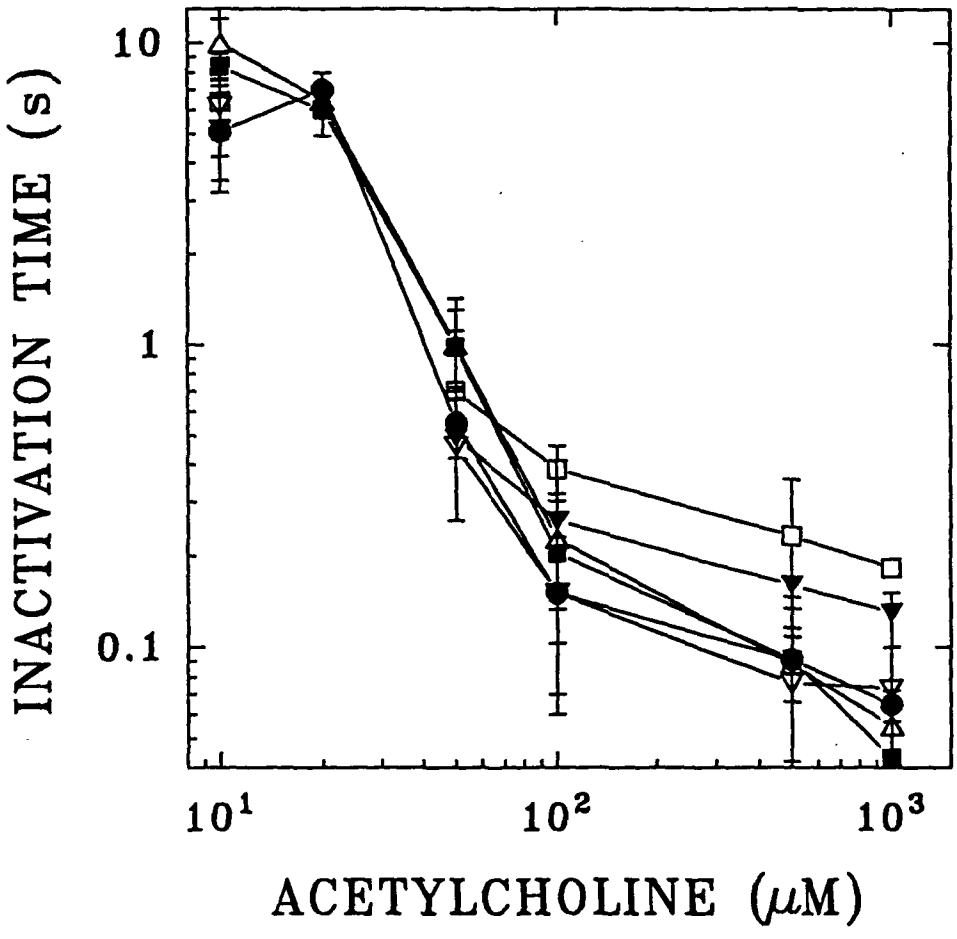

Figure 22. Desensitization of ACh-elicited currents in oocytes injected with AChRα7 receptors. (Δ) AChRα7wt, (■) AChRα7 (S → A), (●) AChRα7 (S → N), (▽) AChRα7 (S → D), (▼) AChRα7 (S → Q), and (□) AChRα7 (S → E). Ooocytes were held at - 80 mV and currents were evoked perfusing the oocytes with indicated ACh concentrations. Inactivation time denotes the decay time of the peak current to 50% of its maximum value. Values are given as means ± SD with N ≥ 10.

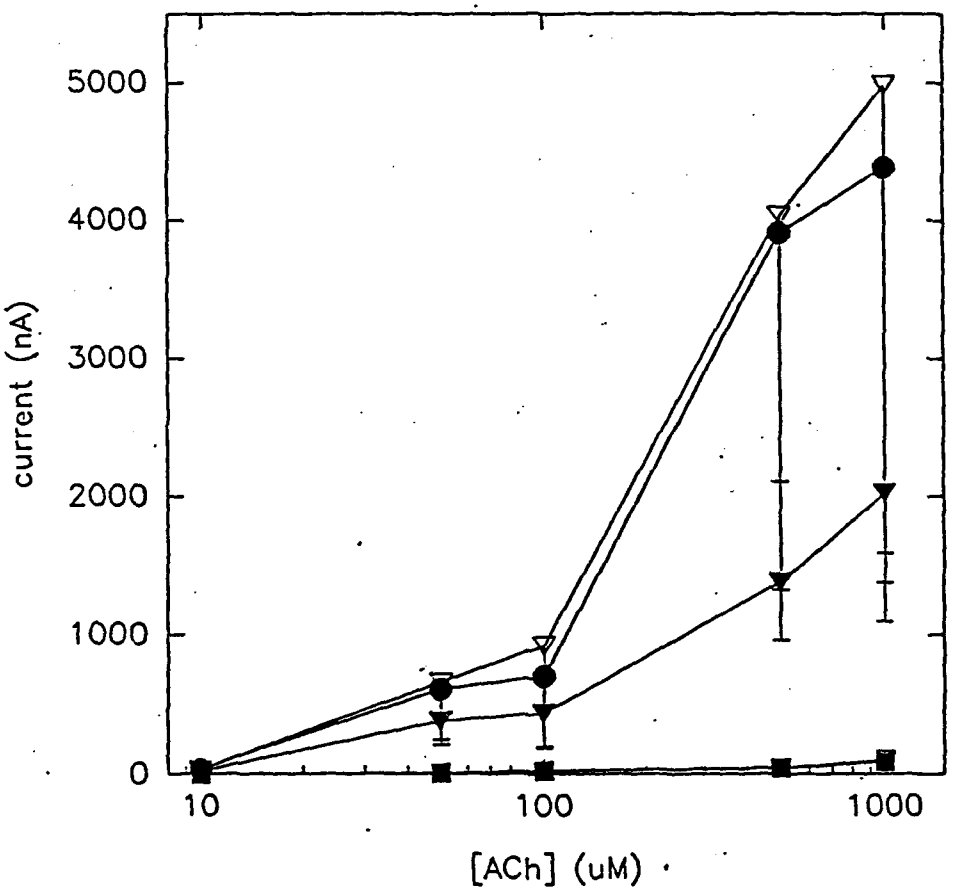

Figure 23. ACh-elicited currents in oocytes expressing neuronal AChRα7 receptors and its chimeras. (V) AChRα7 wild-type, (●) AChRα7α7, (▼), AchRα7 (deletion), (□) ACHRα7 (δ) and (■) AChRα7 (β). Oocytes were held at -80 mV. Current values are given as means ± SD with N ≥ 5. Other conditions as described in Methods.

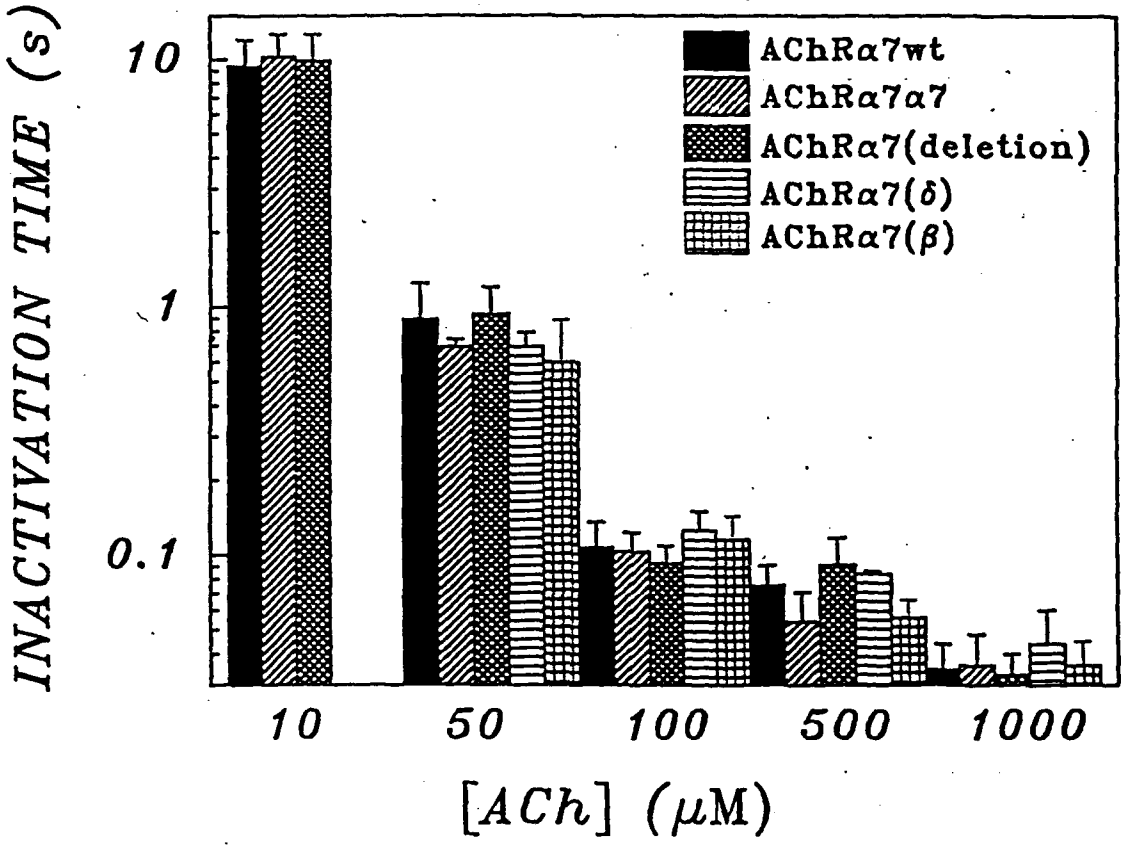

Figure 24. Inactivation of ACh-evoked currents in oocytes expressing neuronal AChRα7. Oocytes were held at -80 mV and currents elicited at indicated ACh concentrations. Values are given as means ± SD with N ≥ 5. Other conditions as described in Fig. 23.

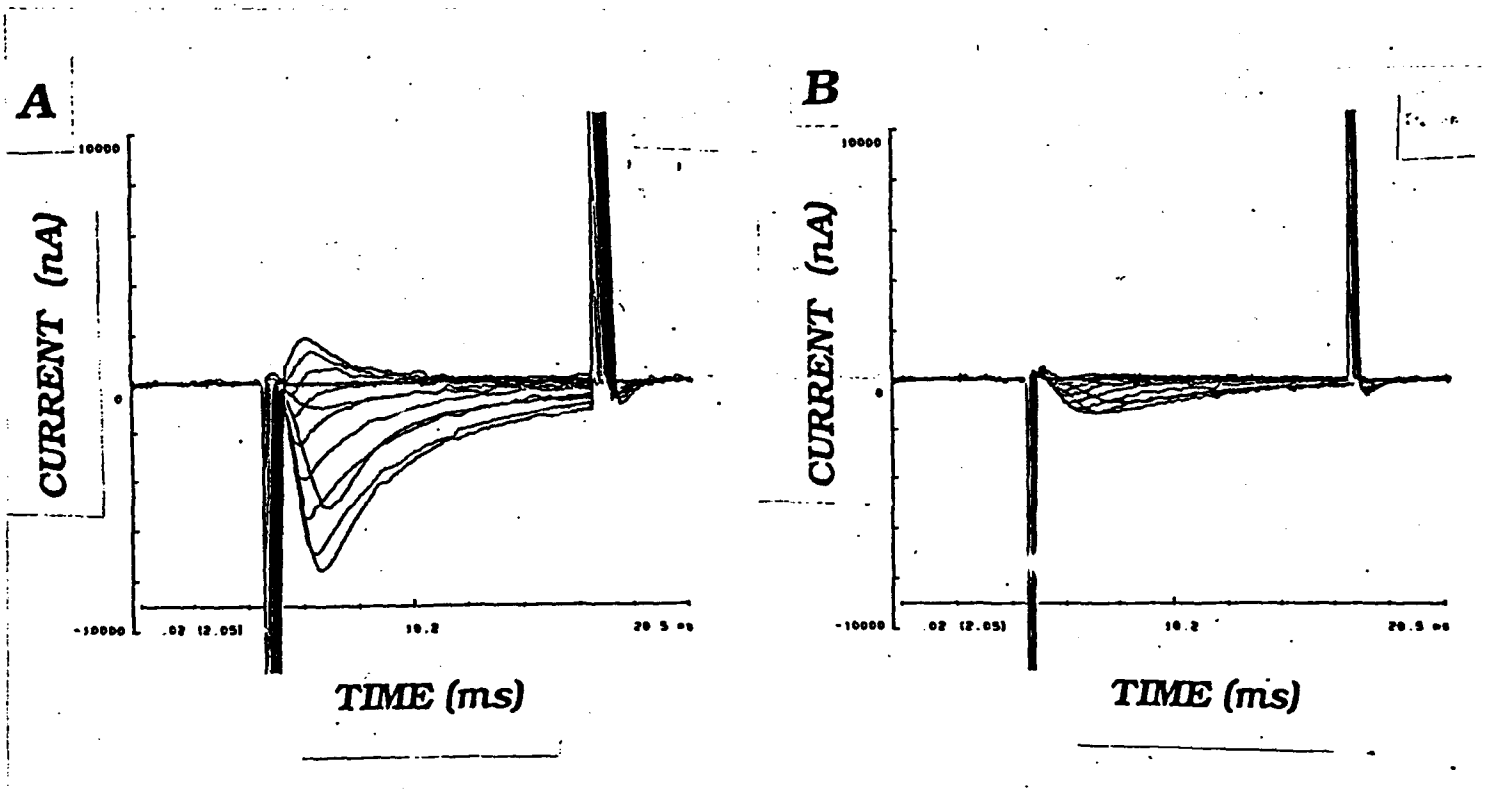

Figure 25. Effect of phorbolesters activator of protein kinase C on the rat brain sodium channel expressed in *Xenopus* oocytes. Currents were recorded under voltage clamp conditions. A family of sodium currents elicited by 15-ms voltage steps from a holding potential of -90 mV to a series of test potentials ranging from -70 mV to 80mV in 10mV increments. Currents were filtered at 1 kHz. Capacitative transients at the onset and termination of voltage pulse are indicated. A: Control Record; B: After addition of 1 μM TPA and incubation of 40 min with the same oocyte as in A.

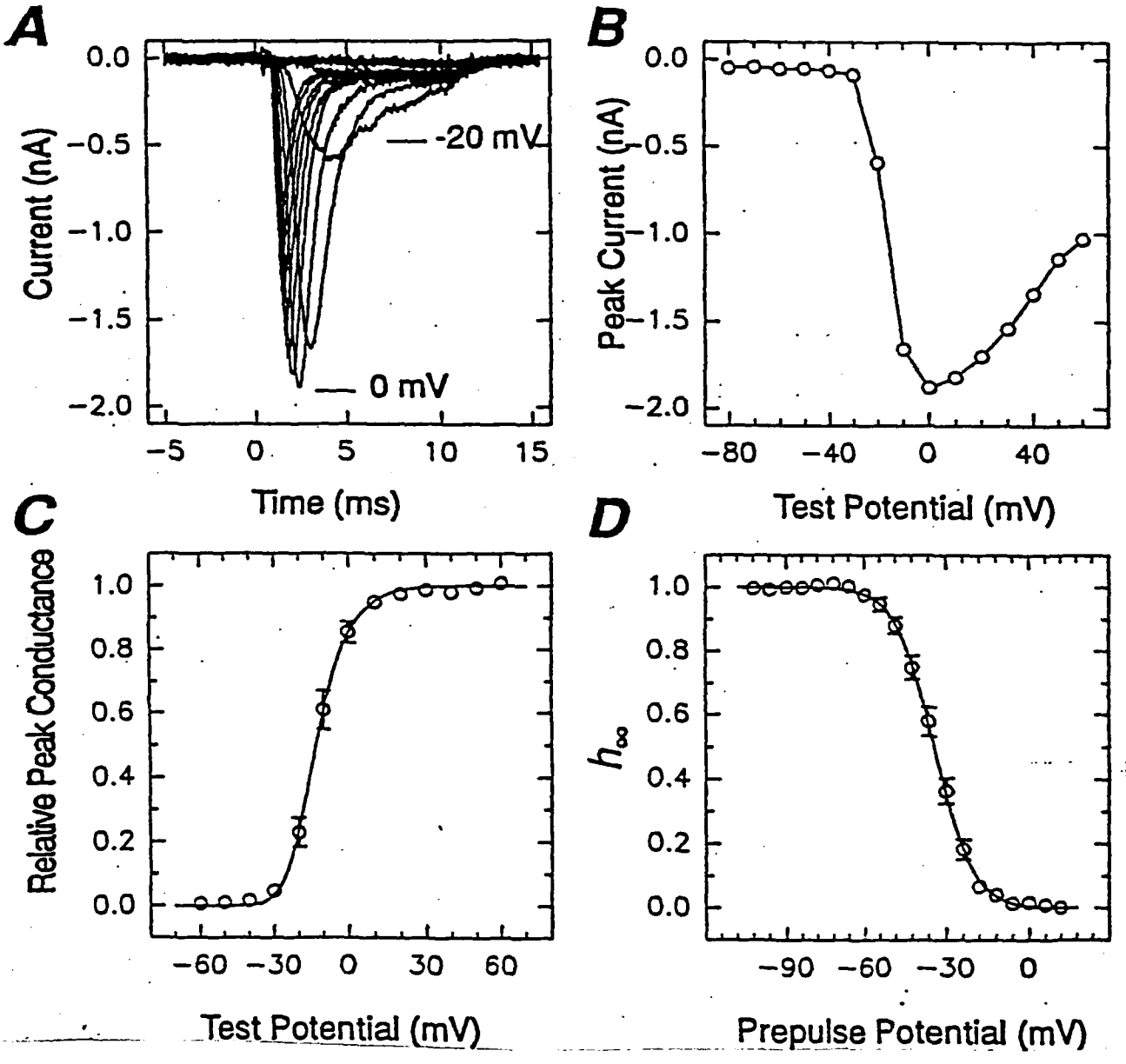

Figure 26. The HBA gene product is a voltage-gated sodium channel. Currents were recorded under CHO cells transfected with HBA DNA. A: Family of sodium currents elicited by 10-ms voltage steps from a holding potential of -100mV. Test potentials ranged from -80mV to 60mV in 10-mV increments. Currents were filtered at 3 kHz. B: Peak currents plotted versus test potential for the same records shown in A. C: Peak conductance-voltage relationship calculated according to $g_{peak}=I_{peak}/(V-V_{Na}^+)$, where V denotes the applied voltage and V_{Na}^+ the Nernst equilibrium potential. Solid line depicts the least-square fit to data points and is given by $g=\{1/[1+\exp(V_{1/2}-V/a)]\}^3$, where $V_{1/2}$ = -24.08 mV and a = 8.3 mV. Each point represents mean+SEM (N=18). D: Steady-state voltage-dependence of inactivation determined using a series of 100 ms prepulses ranging from -102mV to 12 mV followed by a 10 ms test pulse to 0 m V, Peak currents were normalized with respect to the maximum and plotted as a function of prepulse V. Solid line depicts the least-square fit to the data points given by $h_\infty = 1/[1+\exp(V-V_{1/2}/a)]$, where $V_{1/2}$ = -34.07mV and a = 6.85 mV. Each point contains data from a minimum of 6 and a maximum of 17 experiments (mean ±SEM).

Appendix C. Publications, including Abstracts, that resulted from this funding.

Luther, M.A., R. Schoepfer, P. Whiting, B. Casey, Y. Blatt, M.S. Montal, M. Montal and J. Lindstrom. A muscle acetylcholine receptor is expressed in the human cerebellar medulloblastoma cell line TE671. **J. Neurosci.** 9:1082-1096 (1989).

Keller, B.U., M.S. Montal, R.P. Hartshorne and M. Montal. Two–dimensional probability density analysis of single channel currents from reconstituted acetylcholine receptors and sodium channels. **Arch. Biochem. Biophys.** 276:47-54 (1990).

Montal, M. Molecular anatomy and molecular design of channel proteins **FASEB J.** 4:2623-2635 (1990).

Bechinger, B., Y. Kim, L.E. Chirlian, J. Gesell, J.-M. Neumann, M. Montal, J. Tomich, M. Zasloff and S.J. Opella. Orientations of amphipathic helical peptides in membrane bilayers determined by solid–state NMR spectroscopy. **J. Biomol. NMR** 1:167-173. (1991).

Tomich, J.M., A. Grove, T. Iwamoto, S. Marrer, M.S. Montal and M. Montal. Design principles and chemical synthesis of oligomeric channel proteins. In: *Membrane Electrochemistry*. I. Vodyanoy and M. Blank, ed(s). American Chemical Society, ACS Publishing, In press (1991).

Grove, A., T. Iwamoto, M.S. Montal, J.M. Tomich and M. Montal. Synthetic peptides and proteins as models for pore-forming structure of channel proteins. In: *Methods in Enzymology: Ion Channels*. Vol. 207. B. Rudy and L.E. Iverson, ed(s). Academic Press, New York, pp. 510-525 (1992).

Grove, A., J.M. Tomich and M. Montal. A molecular blueprint for the pore–forming structure of voltage–gated calcium channels. **Proc. Natl. Acad. Sci. USA.** 88:6418-6422 (1991).

Ware, D.H., S.C. Lee, C.M.I. Ahmed, C.B. Wagner-Mcpherson, G.A. Evans and M. Montal. Molecular cloning, sequence analysis and chromosomal localization of genes encoding voltage gated sodium channels from human brain cortex. **Soc. Neurosci.** 17(1):952 (1991).

Grove, A., T. Iwamoto, M.S. Montal, G.L. Reddy, S. Marrer, J.M. Tomich, and M. Montal. Towards a unifying structural motif for the pore-forming structure of channel proteins. In: *Biotechnology of Cell Regulation*. R. Verna and Y. Nishizuka, ed(s). Serono Symposia, Raven Press, New York, pp. 89-102 (1991).

Ferrer-Montiel, A.V, M.S. Montal., M. Díaz-Muñoz and M. Montal. Agonist-independent activation of acetylcholine receptor channels by protein kinase A phosphorylation. **Proc. Natl. Acad. Sci. USA** 88:10213-10217 (1991).

Sun, W., A.V. Ferrer-Montiel, A.F. Schinder, J.P. McPherson, G.A. Evans and M. Montal. Molecular cloning, chromosomal mapping, and functional expression of human brain glutamate receptors. **Proc. Natl. Acad. Sci. USA** 89:1443-1447 (1992).

Ferroni, S., R. Planells-Cases, C.M.I. Ahmed and M. Montal. Expression of a genomic clone encoding a brain potassium channel in mammalian cells using lipofection. **Eur. Biophys. J.** 21:185-191 (1992).

Grove, A., J.M. Tomich and M. Montal. Molecular design of oligomeric channel proteins. In: *Genetic Engineering*, Principles and Methods. Vol. 14, pp. 163-184, J.K. Setlow, ed. Plenum Press, New York (1992).

Sun, W., A.V. Ferrer-Montiel, A.F. Schinder, J.P. McPherson, G.A. Evans and M. Montal. Molecular cloning of cDNAs encoding glutamate receptors from human brain cortex. **Biophys. J.** 61:A105 (1992).

Ferroni, S., R. Planells-Cases, C.M.I. Ahmed and M. Montal. Expression of channel clones in mammalian cells by lipofection. **Biophys. J.** 61:A250 (1992).

Grove, A., J.M. Tomich, T. Iwamoto, G.L. Reddy, S. Marrer, M.S. Montal and M. Montal. Design and synthesis of four-helix bundle channel proteins. **J. Cell. Biochem.** 16D:115 (1992).

Ahmed, C.M.I., D.H. Ware, S.C. Lee, C.D. Patten, A.V. Ferrer-Montiel, A.F. Schinder, J.P. McPherson, K. Wagner-McPherson, J.J. Wasmuth, G.A. Evans and M. Montal. Primary structure, chromosomal localization and functional expression of a voltage gated sodium channel from human brain. **Proc. Natl. Acad. Sci. USA** 89:8220-8224 (1992).

Grove, A., J.M. Tomich, T. Iwamoto and M. Montal. Molecular design of a dihydropyridine-sensitive calcium channel protein. In: *Miles Symposium on Nimodipine.* On calcium channel antagonists in the central nervous system. Proceedings of the Santa Fe, New Mexico Symposium, A. Scriabine, ed. In press (1992).

Leopold, P.E., M. Montal and J.N. Onuchic. The kinetic structure of compact conformation space. **Biophys. J.** 61:A131 (1992).

Leopold, P.E., M. Montal and J.N. Onuchic. Protein folding funnels: A kinetic approach to the sequence-structure relationship. **Proc. Natl. Acad. Sci. USA** 89:8721-8725 (1992).

Díaz-Muñoz, M., A.V. Ferrer-Montiel and M. Montal. Tyrosine phosphorylation regulates the channel activity of the nicotinic acetylcholine receptor. Biophysical Society Annual Meeting, Washington, D.C., February 14-18, 1993 (1992).

Díaz-Muñoz, M., A.V. Ferrer-Montiel, N.K. Tonks and M. Montal. Concerted modulation of acetylcholine receptor channel gating by ligand binding and tyrosine phosphorylation. **Proc. Natl. Acad. Sci. USA**, Submitted (1992).

Appendix D. Personnel receiving pay from the contract support.

Name	Job Title	Period Paid
Cervantes, G.	Development Technician I	10/90-11/90; 2/91; 4/91; 8/91
Chmelar, R.	Assistant II	9/89-11/89
Díaz-Muñoz, M.	Postgraduate Researcher I	1/91-6/92
Ferrer-Montiel, A.V.	Postgraduate Researcher III	11/91; 8/92-10/92
Furse, J.	Computer Assistant III	8/91-10/92
Grove, A.	Postgraduate Researcher V	9/92
Hernandez, R.	Assistant II	1/91-6/91; 9/91-11/91
Hoang, D.	Assistant II	2/90-6/90; 9/90-11/91; 7/92-10/92
Lee, S.	Staff Research Associate I	7/89-10/92
Martinez, D.	Assistant II	9/89-9/90
Montal, M.	Principal Investigator	6/89-9/89
Planells-Cases, R.	Lab Assistant I	10/90-8.92
Schiffer, J.	Research Assistant	7/92-10/92
Schinder, A.	Research Assistant	8/90; 10/90-11/91; 7/92-8/92
Sun, W.	Research Assistant	9/91-1/92; 7/92-8/92
Tran, L.	Assistant II	10/90-1/91; 6/92-9/92
Xu, S.	Postgraduate Researcher II	7/89-12/91
Ware, D.	Staff Research Associate II	9/89-12/91